Inorganic Chemistry
Article

Inorg. Chem. **2009**, *48*, 7613–7629 **7613**
DOI: 10.1021/ic900840w

Energy Transfers in Monomers, Dimers, and Trimers of Zinc(II) and Palladium(II) Porphyrins Bridged by Rigid Pt-Containing Conjugated Organometallic Spacers

Diana Bellows,[†] Shawkat M. Aly,[†] Claude P. Gros,[‡] Maya El Ojaimi,[‡] Jean-Michel Barbe,[‡] Roger Guilard,*[,‡] and Pierre D. Harvey*[,†]

[†]*Département de chimie, Université de Sherbrooke, Sherbrooke, Québec, Canada, and* [‡]*ICMUB (UMR 5260), Université de Bourgogne, Dijon, France*

Received February 3, 2009

A series of linear monomers (spacer−M(P)), dimers (M(P)−spacer−M′(P)), and trimers (M(P)−spacer−M′(P)−spacer−M(P)) of spacer/metalloporphyrin systems (M′ = Zn, M = Zn, Pd, P = porphyrin, and spacer = *trans*-$C_6H_4C{\equiv}CPtL_2C{\equiv}CC_6H_4$- (L=$PEt_3$)) including mixed metalloporphyrin compounds, were synthesized and characterized. The S_1 and T_1 energy transfers Pd(P)*→Zn(P) occur with rates of $\sim 2 \times 10^9$ s^{-1}, S_1, and 0.15×10^3 (slow component) and 4.3×10^3 s^{-1} (fast component), T_1. On the basis of a literature comparison with a related dyad, the Pt atom in the conjugated chain slows down the transfers. The excitation in the absorption band of the *trans*-$C_6H_4C{\equiv}CPtL_2C{\equiv}CC_6H_4$-spacer in the 300−360 nm range also leads to T_1 energy transfer (spacer* → M(P); M = Zn, Pd) with rates of 10^4 s^{-1}.

Introduction

Excited state energy transfers and energy delocalization (exciton) are the most basic non-radiative processes that secure the energy migration across the photosynthetic membranes in bacteria, algae, and plants (antenna effect).[1−11] Several research groups have successfully used chemical models to mimic these photophysical processes.[12−15] Among the most spectacular natural devices, one finds the LH II (light harvesting system II; Scheme 1) of the purple photosynthetic bacteria.[16−34] This device is also one of the most

*To whom correspondence should be addressed. E-mail: roger.guilard@u-bourgogne.fr (R.G.), pierre.harvey@usherbrooke.ca (P.D.H.). Phone: 33 (0)3 80 39 61 11 (R.G.), 819-821-7092 (P.D.H.). Fax: 819-821-8017 (P.D.H.).

(1) Ferreira, K. N.; Iverson, T. M.; Maghlaoui, K.; Barber, J.; Iwata, S. *Science* **2004**, *303*, 1831–1838.
(2) Jordan, P.; Fromme, P.; Witt, H. T.; Klukas, O.; Saenger, W.; Krauss, N. *Nature* **2001**, *411*, 909–917.
(3) Koepke, J.; Hu, X.; Muenke, C.; Schulten, K.; Michel, H. *Structure* **1996**, *4*, 581–597.
(4) Küehlbrant, W.; Wang, D. N.; Fujiyoshi, Y. *Nature* **1994**, *367*, 614–621.
(5) Li, Y.-F.; Zhou, W.; Blankenship, R. E.; Allen, J. P. *J. Mol. Biol.* **1997**, *271*, 456–471.
(6) Liu, Z.; Yan, H.; Wang, K.; Kuang, T.; Zhang, J.; Gui, L.; An, X.; Chang, W. *Nature* **2004**, *428*, 287–292.
(7) McDermott, G.; Prince, S. M.; Freer, A. A.; Hawthornthwaite-Lawless, A. M.; Papiz, M.; Cogdell, R. J.; Isaacs, N. W. *Nature* **1995**, *374*, 517–521.
(8) McLuskey, K.; Prince, S. M.; Cogdell, R. J.; Isaacs, N. W. *Biochemistry* **2001**, *4*, 8783–8789.
(9) Roszak, A. W.; Howard, T. D.; Southall, J.; Gardiner, A. T.; Law, C. J.; Isaacs, N. W.; Cogdell, R. J. *Science* **2003**, *302*, 1969–1972.
(10) Schirmer, T.; Bode, W.; Huber, R. *J. Mol. Biol.* **1987**, *196*, 677–696.
(11) Tronrud, D. E.; Schmid, M. F.; Matthews, B. W. *J. Mol. Biol.* **1986**, *188*, 443–454.
(12) Hwang, I.-W.; Park, M.; Ahn, T. K.; Yoon, Z. S.; Ko, D. M.; Kim, D.; Ito, F.; Ishibashi, Y.; Khan, S. R.; Nagasawa, Y.; Miyasaka, H.; Ikeda, C.; Takahashi, R.; Ogawa, K.; Satake, A.; Kobuke, Y. *Chem. Eur. J.* **2005**, *11*, 3753–3761.
(13) Kobuke, Y. *Struct. Bonding* (*Berlin*) **2006**, *121*, 49–104.
(14) Li, J.; Ambroise, A.; Yang, S. I.; Diers, J. R.; Seth, J.; Wack, C. R.; Bocian, D. F.; Holten, D.; Lindsey, J. S. *J. Am. Chem. Soc.* **1999**, *121*, 8927–8940.
(15) Satake, A.; Tanaka, H.; Hajjaj, F.; Kawai, T.; Kobuke, Y. *Chem. Commun.* **2006**, *24*, 2542–2544.
(16) Armitage, J. P. In *Comprehensive Series in Photosciences*; Häder, D.-P., Lebert, M., Eds.; Elsevier Science: New York, 2001; Vol. *1*, pp 117−150.
(17) Blankenship, R. E. *Trends Plant Sci.* **2001**, *6*, 4–6.
(18) Cogdell, R. J.; Gardiner, A. T.; Roszak, A. W.; Law, C. J.; Southall, J.; Isaacs, N. W. *Photosynth. Res.* **2004**, *81*, 207–214.
(19) Cogdell, R. J.; Howard, T. D.; Bittl, R.; Schlodder, E.; Geisenheimer, I.; Lubitz, W. *Philos. Trans. R. Soc. London, Ser. B* **2000**, *355*, 1345–1349.
(20) Cogdell, R. J.; Howard, T. D.; Isaacs, N. W.; McLuskey, K.; Gardiner, A. T. *Photosynth. Res.* **2002**, *74*, 135–141.
(21) Cogdell, R. J.; Isaacs, N. W.; Freer, A. A.; Arrelano, J.; Howard, T. D.; Papiz, M. Z.; Hawthornthwaite-Lawless, A. M.; Prince, S. *Prog. Biophys. Mol. Biol.* **1997**, *68*, 1–27.
(22) Cogdell, R. J.; Southall, J.; Gardiner, A. T.; Law, C. J.; Gall, A.; Roszak, A. W.; Isaacs, N. W. *C. R. Acad. Sci. Paris, Chim.* **2006**, *9*, 201–206.
(23) Fleming, G. R. *Curr. Opin. Struct. Biol.* **1997**, *7*, 738–748.
(24) Fyfe, P. K.; Jones, M. R. *Biochem. Soc. Trans.* **2005**, *33*, 924–930.
(25) Katilius, E.; Woodbury, N. W. In *Encyclopedia of Biological Chemistry*; Lennarz, W. J., Lane, M. D., Eds.; Elsevier: New York, 2004; Vol. *3*, pp 582−585.
(26) Koyama, Y.; Rondonuwu, F. S.; Fujii, R.; Watanabe, Y. *Biopolymers* **2004**, *74*, 2–18.
(27) Kyndt, J. A.; Meyer, T. E.; Cusanovich, M. A. *Photochem. Photobiol. Sci.* **2004**, *3*, 519–530.
(28) Law, C. J.; Roszak, A. W.; Southall, J.; Gardiner, A. T.; Isaacs, N. W.; Cogdell, R. J. *Mol. Membr. Biol.* **2004**, *21*, 183–191.
(29) Meyer, T. E.; Cusanovich, M. A. *Photosynth. Res.* **2003**, *76*, 111–126.
(30) Polivka, T.; Sundström, V. *Chem. Rev.* **2004**, *104*, 2021–2072.
(31) Robert, B.; Cogdell, R. J.; van Grondelle, R. In *Advances in Photosynthesis and Respiration*; Springer: Berlin, 2003; Vol. *13*, pp 169−194.
(32) Scholes, G. D.; Fleming, G. R. *J. Phys. Chem. B* **2000**, *104*, 1854–1868.
(33) Sundström, V.; Pullerits, T.; van Grondelle, R. *J. Phys. Chem. B* **1999**, *103*, 2327–2346.
(34) Yang, M.; Agarwal, R.; Fleming, G. R. *J. Photochem. Photobiol., B* **2001**, *142*, 107–119.

Published on Web 07/22/2009

Scheme 1. (Top Left) Drawing of LH II Showing the B850 Network, the Non-Interacting B800s, and the Carotenoids; [a] (Top Right) Drawing of the Local Environment of the Carotenoids (in Black) and the B800 and B850 Units Stressing the Downhill S_1 Energy Transfers and the Possible Slightly Uphill Transfers (Carotenoid → B850); (Bottom) Structures of the Bacteriochlorophyll *a* and of the Carotenoid

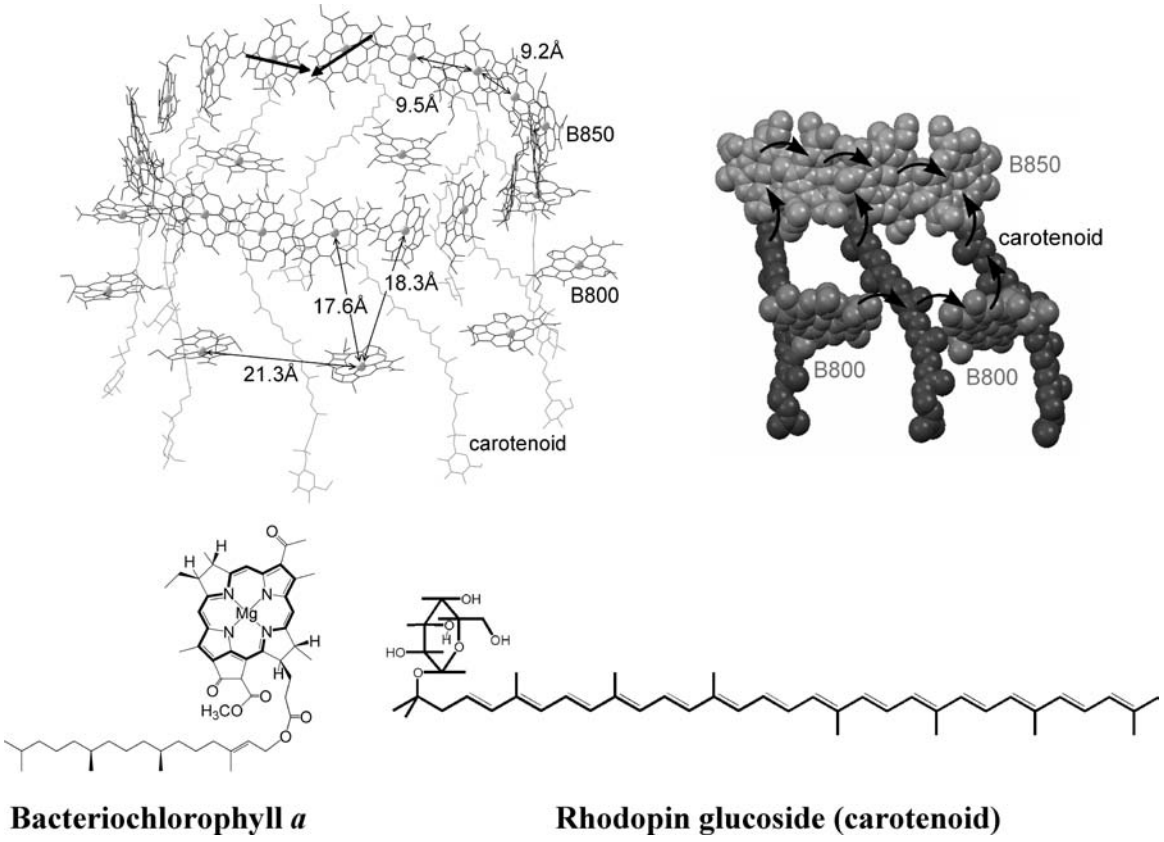

[a] The quasi-parallel arrows represent the transition moments of two B850 units.

well-documented among the photosynthetic bacteria.[35,36] In this case, the singlet state energy migration from B800 → B850 (B = bacteriochlorophyll *a*) systems occurs in the 1 ps time scale despite the long center-to-center separation (∼18 Å).[37] It is strongly believed that the auxiliary carotenoid is used as a relay between the donor and acceptor.

Inspired by the observation that S_1 energy transfer between a donor and an acceptor that are not conjugated is possible, even when separated by 18 Å or so, it appears convenient to design a series of dyads composed of porphyrinoids that exhibit similar features as that shown above in the natural system (B800−B850). In that respect, we now wish to report a series of dimers and trimers (Chart 1) for the investigation of S_1 and T_1 energy transfers in unconjugated donor-spacer-acceptor systems rigidly held by a conjugated organometallic fragment ($-C_6H_4C{\equiv}CPtL_2C{\equiv}CC_6H_4-$). The donor and acceptor are very poorly conjugated owing the quasi right angle formed by the metalloporphyrin ring and phenyl group. The choice of a heavy metal (Pt) is driven by the opportunity to also investigate the T_1 state behavior (a state whose population is enhanced by heavy atom effect), by the dimension of the atom allowing to reach the desired targeted donor−acceptor separation, and by the fact that π-conjugation is still possible across the spacer from the presence of the d_{xy} metal orbital. Energy migrations in the S_1 state are noted. This conclusion bears an important consequence on the anticipated antenna effect in one-dimensional (1-D) materials built upon these dyads and monodispersed oligomers (Chart 1).

Experimental Section

Materials. The porphyrin precursors, *a,c*-biladiene and 3,3′-diethyl-4,4′-dimethyldipyrromethane, were synthesized as previously reported.[38] *cis*-Dichlorobis(triethylphosphine)-platinum(II), *trans*-dichlorobis(triethylphosphine)platinum(II) were prepared according to standard procedures.[39,40] The following materials were purchased from commercial suppliers: DDQ (dichlorodicyanoquinone; Aldrich), triethylphosphine (Aldrich), diisopropylamine (Aldrich), phenylacetylene (Aldrich), copper(I) iodide (Aldrich), [(trimethylsilyl)ethynyl]benzaldehyde (Aldrich), dichloromethane (EMD), platinum(II) chloride (Strem), potassium carbonate (Fisher), ether (ACP), hexane (ACP), ethanol (Commercial Alcohols inc.). All the solvents were purified according to literature procedures.[41] The coupling reactions were performed under argon using Schlenk techniques, with flame-dried reaction vessels before use. Silica gel (Merck; 70−120 μm) was used for column chromatography. Analytical thin layer

(35) Bertini, I.; Gray, H. B.; Stiefel, E. I.; Valentine, J. S. In *Biological Inorganic Chemistry Structure and Reactivity*; Stiefel, J. E., Ed.; University Science Books: Sausalito, CA, 2007; pp 305−316.
(36) Nelson, D. L.; Cox, M. M. In *Lehninger Principles of Biochemistry*; Ahr, K., Ryan, M., O'Neil, J., Wong, V., Ciprioni, J., Mays, M., Tymoczko, N. E., Eds.; W. H. Freeman and Company: New York, 2005; pp 725−735.
(37) Harvey, P. D.; Stern, C.; Gros, C. P.; Guilard, R. *J. Inorg. Biochem.* **2008**, *102*, 395–405.
(38) Guilard, R.; Gros, C. P.; Bolze, F.; Jérôme, F.; Ou, Z. P.; Shao, J. G.; Fischer, J.; Weiss, R.; Kadish, K. M. *Inorg. Chem.* **2001**, *40*, 4845–4855.
(39) Kharasch, M. S.; Seyler, R. C.; Mayo, F. R. *J. Am. Chem. Soc.* **1938**, *60*, 882–884.
(40) Parshall, G. W. *Inorg. Synth.* **1970**, *12*, 26–33.
(41) Perrin, D. D.; Armarego, W. L. F.; Perrin, D. R. *Purifications of laboratory chemicals*; Pergamon Press: Oxford, 1966.

Chart 1

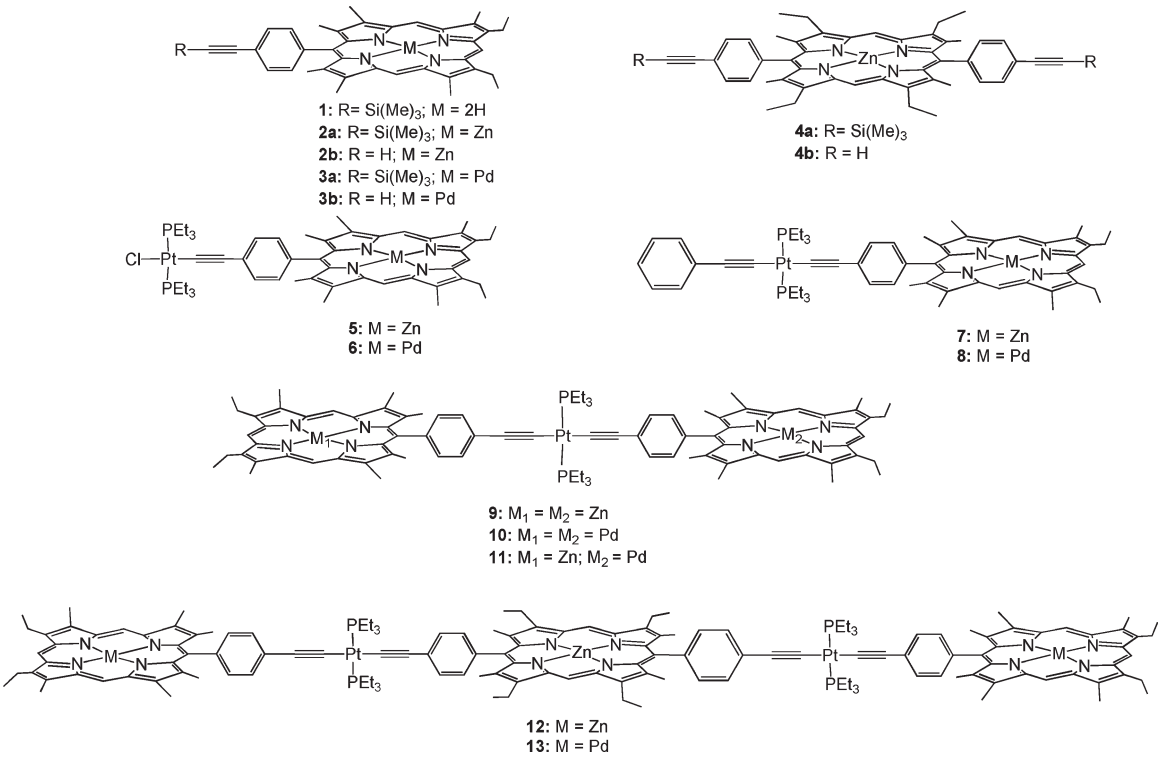

chromatography was performed using Merck 60 F_{254} silica gel (precoated sheets, 0.2 mm thick). All the reactions were monitored by thin-layer chromatography and UV−visible spectroscopy.

5-[4-(Trimethylsilyl)ethynylphenyl]-13,17-diethyl-2,3,7,8,12,18-hexamethyl-porphyrin (1). A mixture of 2.01 g (9.93 mmol) of 4-[(trimethylsilyl)ethynyl]-benzaldehyde and 4.00 g (6.64 mmol) of *a,c*-biladiene dihydrobromide[38] was dissolved in 500 mL of hot absolute ethanol. *p*-Toluenesulfonic acid (8.0 g) in 100 mL of ethanol was slowly added over 12 h, and the mixture was stirred under reflux for 48 h. The mixture was cooled to room temperature, and the solution was evaporated under vacuum. The residue was dissolved in dichloromethane (500 mL), neutralized with a saturated solution of $NaHCO_3$, and then washed thoroughly three times with 1 L of water. The organic phase was dried over $MgSO_4$ and filtered, the solvent was removed in vacuo. The residue was purified by silica column chromatography (CH_2Cl_2 as eluent). The second fraction was collected, concentrated, and crystallized from CH_2Cl_2/MeOH to yield the title compound (1.9 g; 30% yield) as a purple solid. ^{1}H NMR ($CDCl_3$) δ (ppm): 10.36 (s, 2H, H-*meso*), 10.20 (s, 1H, H-*meso*), 8.29 (d, 2H, $^3J_{H-H}$ = 8 Hz, H-Phenyl), 8.04 (d, 2H, $^3J_{H-H}$ = 8 Hz, H-Phenyl), 3.96 (q, 4H, $^3J_{H-H}$ = 7.6 Hz, CH_2), 3.56 (s, 6H, CH_3), 3.33 (s, 6H, CH_3), 2.32 (s, 6H, CH_3), 2.00 (t, 6H, $^3J_{H-H}$ = 7.6 Hz, CH_3), 1.35 (s, 9H, Si-CH_3), −0.85 (s, 1H, NH), −1.93 (s, 1H, NH). HR-MS (MALDI-TOF): m/z = 622.3503 $[M]^{+\bullet}$; 622.3492 calcd for $C_{41}H_{46}N_4Si$. UV−visible (CH_2Cl_2): λ_{max} nm ($\varepsilon \times 10^{-3}$, M^{-1} cm^{-1}) = 405 (188), 500 (10.1), 535 (11.1), 570 (11.0), 620 (3.7).

5-[4-(Trimethylsilyl)ethynylphenyl]-13,17-diethyl-2,3,7,8,12,18-hexamethyl-porphyrin Zinc (2a). 5-[4-(Trimethylsilyl)ethynyl-phenyl]-13,17-diethyl-2,3,7,8,12,18-hexamethylporphyrin **1** (600 mg, 0.964 mmol) and zinc acetate tetrahydrate (317 mg, 1.44 mmol) were dissolved in chloroform (70 mL) and methanol (30 mL) and refluxed for 90 min in the presence of sodium acetate (790 mg, 9.63 mmol). The metalation reaction was monitored by UV−visible spectroscopy and MALDI-TOF mass spectrometry. At the end of the reaction, the solvent was removed in vacuo, and the crude product was dissolved in dichloromethane (100 mL), washed with water (3 × 500 mL), and dried over $MgSO_4$. The solvent was removed in vacuo, and the residue was purified by silica column chromatography (CH_2Cl_2 as eluent). After evaporation, the title compound **2a** was obtained in 86% yield (567 mg) as a red microcrystalline solid. ^{1}H NMR ($CDCl_3$) δ (ppm): 10.07 (s, 2H, H-*meso*), 9.93 (s, 1H, H-*meso*), 8.01 (d, 2H, $^3J_{H-H}$ = 8 Hz, H-Phenyl), 7.88 (d, 2H, $^3J_{H-H}$ = 8 Hz, H-Phenyl), 4.05 (q, 4H, $^3J_{H-H}$ = 7.6 Hz, CH_2), 3.61 (s, 6H, CH_3), 3.52 (s, 6H, CH_3), 2.47 (s, 6H, CH_3), 1.87 (t, 6H, $^3J_{H-H}$ = 7.6 Hz, CH_3), 1.28 (s, 9H, Si-CH_3). MS (MALDI-TOF): m/z = 684.10 $[M]^{+\bullet}$; 684.26 calcd for $C_{41}H_{44}N_4SiZn$. HR-MS (ESI): m/z = 685.2706 $[M + H]^+$; 685.2699 calcd for $C_{41}H_{45}N_4SiZn$, m/z = 707.2539 $[M + Na]^+$; 707.2519 calcd for $C_{41}H_{44}N_4NaSiZn$. UV−visible (CH_2Cl_2): λ_{max} nm ($\varepsilon \times 10^{-3}$, M^{-1} cm^{-1}) = 403 (203), 533 (8.9), 569 (9.9).

5-(4-Ethynylphenyl)-13,17-diethyl-2,3,7,8,12,18-hexamethyl-porphyrin Zinc (2b). To a solution of 5-[4-(2-(trimethylsilyl)-ethynylphenyl]-13,17-diethyl-2,3,7,8,12,18-hexamethymporphyrin zinc **2a** (567 mg, 0.829 mmol) in tetrahydrofuran (THF, 100 mL) was added NBu_4F (4 mL, 4 mmol, 1 M in THF). After the mixture was stirred at room temperature for 12 h, the solution was evaporated under reduced pressure and dissolved in methylene chloride. The solution was washed with a saturated NH_4Cl solution, 3 times with water and dried over anhydrous $MgSO_4$. After purification over a silica plug (CH_2Cl_2 as eluent), the title compound **2b** was isolated in 78% yield (397 mg). ^{1}H NMR ($CDCl_3$) δ (ppm): 9.98 (s, 2H, H-*meso*), 9.80 (s, 1H, H-*meso*), 7.99 (d, 2H, $^3J_{H-H}$ = 7.5 Hz, H-Phenyl), 7.88 (d, 2H, $^3J_{H-H}$ = 7.5 Hz, H-Phenyl), 3.99 (q, 4H, $^3J_{H-H}$ = 7.6 Hz, CH_2), 3.54 (s, 6H, CH_3), 3.48 (s, 6H, CH_3), 3.34 (s, 1H, alcyne), 2.43 (t, 6H, $^3J_{H-H}$ = 7.6 Hz, CH_3), 1.82 (s, 6H, CH_3). MS (MALDI-TOF): m/z = 611.89 $[M]^{+\bullet}$; 612.22 calcd for $C_{38}H_{36}N_4Zn$. HR-MS (ESI): m/z = 613.2311 $[M + H]^+$; 613.2304 calcd for $C_{38}H_{37}N_4Zn$, m/z = 635.2140 $[M + Na]^+$; 635.2124 calcd for $C_{38}H_{36}N_4NaZn$. UV−visible (CH_2Cl_2): λ_{max} nm ($\varepsilon \times 10^{-3}$, M^{-1} cm^{-1}) = 403 (288), 533 (17.2), 569 (19.3).

5-(4-(Trimethylsilyl)ethynylphenyl)-13,17-diethyl-2,3,7,8,12,18-hexamethyl-porphyrin Palladium (3a). 5-(4-(Trimethylsilyl)-ethynylphenyl)-13,17-diethyl-2,3,7,8, 12,18-hexamethylporphyrin **1** (400 mg, 0.642 mmol) and sodium acetate (0.540 g, 6.58 mmol) were dissolved under argon in 80 mL of 1,2-dichloroethane. The mixture was heated at 110 °C. A palladium acetate solution (157 mg, 0.700 mmol in 15 mL of methanol) was slowly added over 90 min, and the metalation reaction was monitored by UV−visible spectroscopy and MALDI-TOF mass spectrometry. The solution was cooled to room temperature, washed 3 times with water and evaporated under reduced pressure. After purification on silica column (CH_2Cl_2 as eluent), the title compound **3a** was isolated in 65% yield (302 mg). ^{1}H NMR ($CDCl_3$) δ (ppm): 10.07 (s, 2H, H-*meso*), 10.01 (s, 1H, H-*meso*), 7.94 (d, 2H, $^3J_{H-H}$ = 8 Hz, H-Phenyl), 7.84 (d, 2H, $^3J_{H-H}$ = 8 Hz, H-Phenyl), 4.02 (q, 4H, $^3J_{H-H}$ = 7.6 Hz, CH_2), 3.46 (s, 6H, CH_3), 2.41 (s, 6H, CH_3), 1.87 (t, 6H, $^3J_{H-H}$ = 7.6 Hz, CH_3), 1.54 (s, 6H, CH_3), 0.40 (s, 9H, Si-CH_3). MS (MALDI-TOF): m/z = 726.00 $[M]^{+\bullet}$; 726.24 calcd for $C_{41}H_{44}N_4PdSi$. HR-MS (ESI): m/z = 727.2457 $[M+H]^+$; 727.2443 calcd for $C_{41}H_{45}N_4PdSi$, m/z = 749.2281 $[M+Na]^+$; 749.2262 calcd for $C_{41}H_{44}N_4NaPdSi$. UV−visible (CH_2Cl_2): λ_{max} nm ($\varepsilon \times 10^{-3}$, M^{-1} cm^{-1}) = 395 (137), 513 (8.0), 547 (24.0).

5-(4-Ethynylphenyl)-13,17-diethyl-2,3,7,8,12,18-hexamethyl-porphyrin Palladium (3b). To a solution of porphyrin palladium **3a** (290 mg, 0.399 mmol) in THF (75 mL) was added NBu_4F (2 mL, 2 mmol, 1 M in THF). After the mixture was stirred at room temperature for 12 h, the solution was evaporated under reduced pressure and dissolved in methylene chloride. The solution was washed with a saturated NH_4Cl solution, 3 times with water and dried over anhydrous $MgSO_4$. After purification over a silica plug (CH_2Cl_2 as), the title compound **3b** was isolated in 96% yield (252 mg). ^{1}H NMR ($CDCl_3$) δ (ppm): 9.97 (s, 2H, H-*meso*), 9.92 (s, 1H, H-*meso*), 7.93 (d, 2H, $^3J_{H-H}$ = 8 Hz, H-Phenyl), 7.82 (d, 2H, $^3J_{H-H}$ = 8 Hz, H-Phenyl), 4.01 (q, 4H, $^3J_{H-H}$ = 7.6 Hz, CH_2), 3.44 (s, 6H, CH_3), 3.29 (s, 1H, alcyne), 2.40 (s, 6H, CH_3), 1.85 (t, 6H, $^3J_{H-H}$ = 7.6 Hz, CH_3), 1.54 (s, 6H, CH_3). HR-MS (ESI): m/z = 655.2074 $[M+H]^+$; 655.2048 calcd for $C_{38}H_{37}N_4Pd$, m/z = 677.1896 $[M+Na]^+$; 677.1867 calcd for $C_{38}H_{36}N_4NaPd$. UV−visible (CH_2Cl_2): λ_{max} nm ($\varepsilon \times 10^{-3}$, M^{-1} cm^{-1}) = 395 (142), 513 (9.8), 547 (26.3).

5,15-Bis[4-(trimethylsilyl)ethynyl]phenyl]-tetraethyl-2,8,12,18-tetramethyl-3,7,13,17-porphyrin Zinc (4a). A solution of 4-[(trimethylsilyl)ethynyl]benzaldehyde (439 mg, 2.17 mmol) and 3,3′-diethyl-4,4′-dimethyldipyrromethane[38] (500 mg, 217 mmol) in 250 mL of CH_2Cl_2 was treated with $BF_3 \cdot OEt_2$ (0.16 mL). After 30 min, DDQ (1.47 g, 6.51 mmol, 3 equiv) and triethylamine (1.5 mL) were added, and the solution was stirred at room temperature for 1 h. After evaporation, the residue was dissolved in a minimum amount of CH_2Cl_2 and passed through an alumina column using CH_2Cl_2 as the solvent. After removing of the solvent, the crude porphyrin and zinc acetate dihydrate (953 mg, 4.34 mmol) were dissolved in $CHCl_3$ (70 mL) and methanol (30 mL) and refluxed for 90 min in the presence of sodium acetate (1.18 g, 8.68 mmol). The metalation reaction was monitored by UV−visible spectroscopy and MALDI-TOF mass spectrometry. At the end of the reaction, the solvent was removed, and the crude product was dissolved in CH_2Cl_2 (100 mL), washed with water (3 × 500 mL), and dried over $MgSO_4$. The solvent was removed in vacuo, and the residue was purified by silica column chromatography (CH_2Cl_2 as the solvent). After evaporation, the title compound **4a** was obtained in 22% yield (423 mg) as a red microcrystalline solid. ^{1}H NMR ($CDCl_3$) δ (ppm): 10.12 (s, 2H, H-*meso*), 7.98 (d, 4H, $^3J_{H-H}$ = 7.5 Hz, H-Phenyl), 7.84 (d, 4H, $^3J_{H-H}$ = 7.5 Hz, H-Phenyl), 3.95 (q, 8H, $^3J_{H-H}$ = 7.6 Hz, CH_2), 2.41 (s, 12H, CH_3), 1.72 (t, 12H, $^3J_{H-H}$ = 7.6 Hz, CH_3), 1.22 (s, 18H, Si-CH_3). HR-MS (MALDI-TOF): m/z = 884.3671 $[M]^{+\bullet}$; 884.3648 calcd for $C_{54}H_{60}N_4Si_2Zn$. UV−visible (CH_2Cl_2): λ_{max} nm ($\varepsilon \times 10^{-3}$, M^{-1} cm^{-1}) = 411 (267), 539 (15.0), 574 (8.0).

5,15-Bis[(4-ethynyl)phenyl]tetraethyl-2,8,12,18-tetramethyl-3,7,13,17-porphyrin Zinc (4b). This compound was prepared in 93% yield (311 mg, 420.36 mmol) as described for **2b** starting from **4a** (400 mg, 452 mmol). ^{1}H NMR ($CDCl_3$) δ (ppm): 10.09 (s, 2H, H-*meso*), 7.96 (d, 4H, $^3J_{H-H}$ = 7.5 Hz, H-Phenyl), 7.81 (d, 4H, $^3J_{H-H}$ = 7.5 Hz, H-Phenyl), 3.91 (q, 8H, $^3J_{H-H}$ = 7.6 Hz, CH_2), 3.26 (s, 2H, alcyne), 2.38 (s, 12H, CH_3), 1.68 (t, 12H, $^3J_{H-H}$ = 7.6 Hz, CH_3). HR-MS (MALDI-TOF): m/z = 740.2891 $[M]^{+\bullet}$; 740.2857 calcd for $C_{48}H_{44}N_4Zn$. UV−visible (CH_2Cl_2): λ_{max} nm ($\varepsilon \times 10^{-3}$, M^{-1} cm^{-1}) = 411 (235), 539 (13.1), 574 (7.1).

***trans*-Chloro-[5-(4-ethynylphenyl)-13,17-diethyl-2,3,7,8,12,18-hexamethyl(metal)-porphyrin]bis(triethylphosphine)platinum(II) (metal = Zn (5), Pd (6)).** CuI (0.6 mg, 0.003 mmol) was added to a mixture of *trans*-$Pt(PEt_3)_2Cl_2$ (87.5 mg, 0.174 mmol) and porphyrin **2b** (0.035 mmol) or **3b** (0.035 mmol) in $CH_2Cl_2/{}^iPr_2NH$ (50 mL, 1:1 v/v). The purple solution was left to stir overnight under inert atmosphere and refluxed, after which all volatiles were removed under reduced pressure. The residue was redissolved in CH_2Cl_2 and washed 3 times with water and dried over K_2CO_3. All solvents were removed under reduced pressure. The residue was dissolved in a minimum amount of CH_2Cl_2 and passed through a silica column using hexane/CH_2Cl_2 (40/60) as the solvents.

5. Yield: 69% (72.4 mg) ^{1}H NMR ($CDCl_3$) δ (ppm): 10.15 (s, 2H, H-*meso*), 10.05 (s, 1H, H-*meso*), 7.88 (d, 2H, $^3J_{H-H}$ = 8.0 Hz, H-Phenyl), 7.61 (d, 2H, $^3J_{H-H}$ = 8.1 Hz, H-Phenyl), 4.10 (q, 4H, $^3J_{H-H}$ = 7.6 Hz, CH_2), 3.64 (s, 6H, CH_3), 3.54 (s, 6H, CH_3), 2.54 (s, 6H, CH_3), 2.26−2.21 (m, 12H, CH_2), 1.89−1.87 (m, 6H, CH_2CH_3), 1.34−1.25 (m, 18H, CH_3). ^{31}P NMR ($CDCl_3$) δ (ppm): 16.23. IR (KBr) ν: 2115.1 cm^{-1} (C≡C). Anal. Calcd (%) for $C_{50}H_{65}ClN_4P_2PtZn$ (1079.95): C 55.61, H 6.07, N 5.19. Found: C 55.33; H 6.36, N 4.91. MS (MALDI-TOF): m/z = 1080.24 $[M]^{+\bullet}$; 1079.95 calcd for $C_{50}H_{65}ClN_4P_2PtZn$. UV−visible (2MeTHF): λ_{max} nm ($\varepsilon \times 10^{-3}$, M^{-1} cm^{-1}) = 328 (27), 411 (302), 540 (18), 576 (11).

6. Yield: 57% (38.9 mg) ^{1}H NMR ($CDCl_3$) δ (ppm): 10.09 (s, 2H, H-*meso*), 10.03 (s, 1H, H-*meso*), 7.84 (d, 2H, $^3J_{H-H}$ = 7.9 Hz, H-Phenyl), 7.59 (d, 2H, $^3J_{H-H}$ = 8.0 Hz, H-Phenyl), 4.04 (q, 4H, $^3J_{H-H}$ = 7.6 Hz, CH_2), 3.59 (s, 6H, CH_3), 3.48 (s, 6H, CH_3), 2.49 (s, 6H, CH_3), 2.25−2.19 (m, 12H, CH_2), 1.90−1.85 (m, 6H, CH_2CH_3), 1.38−1.25 (m, 18H, CH_3). ^{31}P NMR ($CDCl_3$) δ (ppm): 16.23. IR (KBr) ν: 2118.7 cm^{-1} (C≡C). Anal. Calcd (%) for $C_{50}H_{65}ClN_4P_2PtPd$ (1120.98): C 53.57, H 5.84, N 5.00. Found: C 53.85, H 6.09, N 4.81. MS (MALDI-TOF): m/z = 1120.24 $[M]^{+\bullet}$; 1120.98 calcd for $C_{50}H_{65}ClN_4P_2PtPd$. UV−visible (2MeTHF): λ_{max} nm ($\varepsilon \times 10^{-3}$, M^{-1} cm^{-1}) = 320 (32), 400 (265), 515 (22), 548 (53).

***trans*-(Ethynylphenyl)[5-(4-ethynylphenyl)-13,17-diethyl-2,3,7,8,12,18-hexamethyl-(metal)porphyrin]bis(triethylphosphine)-platinum(II) (metal = Zn (7), Pd (8)).** CuI (0.3 mg, 0.002 mmol) was added to a mixture of $[Pt(PEt_3)_2(C{\equiv}CC_6H_4(M(P)))Cl]$ (19.4 mg, 0.0161 mmol) and phenylacetylene (0.00180 mL, 0.0177 mmol) in $CH_2Cl_2/{}^iPr_2NH$ (50 mL, 1:1 v/v). The purple solution was left to stir overnight under inert atmosphere and refluxed, after which all volatiles were removed under reduced pressure. The residue was redissolved in CH_2Cl_2 and washed 3 times with water and dried over K_2CO_3. All solvents were removed under reduced pressure, and the residue was dissolved in a minimum amount of CH_2Cl_2 and filtered through a silica column using hexane/CH_2Cl_2 (40/60).

7. Yield: 60% (21.8 mg) ^{1}H NMR ($CDCl_3$) δ (ppm): 10.02 (s, 2H, H-*meso*), 9.84 (s, 1H, H-*meso*), 7.85 (d, 2H, $^3J_{H-H}$ = 7.7 Hz, H-Phenyl), 7.65 (d, 2H, $^3J_{H-H}$ = 7.8 Hz, H-Phenyl), 7.35 (m, 3H, $^3J_{H-H}$ = 7.2 Hz, H-Phenyl), 7.26 (d, 2H, $^3J_{H-H}$ = 6.8 Hz, H-Phenyl), 4.00 (q, 4H, $^3J_{H-H}$ = 7.6 Hz, CH_2), 3.57 (s, 6H, CH_3), 3.50 (s, 6H, CH_3), 2.53 (s, 6H, CH_3), 2.40−2.31 (m, 12H, CH_2), 1.86−1.81 (m, 6H, CH_2CH_3), 1.42−1.31 (m, 18H, CH_3). ^{31}P NMR

($CDCl_3$) δ (ppm): 12.44. IR (KBr) ν: 2107.5 cm^{-1} (C≡C). Anal. Calcd (%) for $C_{58}H_{70}N_4P_2PtZn$ (1145.62): C 60.81, H 6.16, N 4.89. Found: C 61.09, H 6.31, N 4.55. MS (MALDI-TOF): m/z = 1145.42 $[M]^{+\bullet}$; 1145.62 calcd for $C_{58}H_{70}N_4P_2PtZn$. UV−visible (2MeTHF): λ_{max} nm ($\varepsilon \times 10^{-3}$, M^{-1} cm^{-1}) = 335 (26), 412 (210), 540 (10), 575 (6).

8. Yield: 45% (10.0 mg) ^1H NMR ($CDCl_3$) δ (ppm): 10.07 (s, 2H, H-*meso*), 10.01 (s, 1H, H-*meso*), 7.81 (d, 2H, J_{H-H} = 7.8 Hz, H-Phenyl), 7.62 (d, 2H, J_{H-H} = 7.8 Hz, H-Phenyl), 7.34 (m, 3H, J_{H-H} = 7.5 Hz, H-Phenyl), 7.23 (d, 2H, J_{H-H} = 6.8 Hz, H-Phenyl), 4.03 (q, 4H, $^3J_{H-H}$ = 7.6 Hz, CH_2), 3.57 (s, 6H, CH_3), 3.47 (s, 6H, CH_3), 2.49 (s, 6H, CH_3), 2.38−2.30 (m, 12H, CH_2), 1.90−1.84 (m, 6H, CH_2CH_3), 1.54−1.32 (m, 18H, CH_3). ^{31}P NMR ($CDCl_3$) δ (ppm): 12.44. IR (KBr) ν: 2106.1 cm^{-1} (C≡C). Anal. Calcd (%) for $C_{58}H_{70}N_4P_2PtPd$ (1186.64): C 58.70, H 5.95, N 4.72. Found: C 58.46, H 5.69, N 5.07. MS (MALDI-TOF): m/z = 1186.37 $[M]^{+\bullet}$; 1186.64 calcd for $C_{58}H_{70}N_4P_2$-PtPd. UV−visible (2MeTHF): λ_{max} nm ($\varepsilon \times 10^{-3}$, M^{-1} cm^{-1}) = 328 (40), 396 (211), 515 (17), 548 (43).

***trans*-Bis[5-(4-ethynylphenyl)-13,17-diethyl-2,3,7,8,12,18-hexamethyl(metal)-porphyrin]bis(triethylphosphine)platinum(II) (metal = Zn (9), Pd (10)), and *trans*-[(5-(4-Ethynylphenyl)-13,17-diethyl-2,3,7,8,12,18-hexamethyl(palladium(II))-porphyrin)-[(5-(4-ethynylphenyl)-13,17-diethyl-2,3,7,8,12,18-hexamethyl-(zinc(II))-porphyrin)]bis(triethylphosphine)platinum(II) (11).** CuI (1.5 mg, 0.0080 mmol) was added to a mixture of *trans*-Pt-$(PEt_3)_2Cl_2$ (38.7 mg, 0.0770 mmol) and the corresponding porphyrin (0.154 mmol) in $CH_2Cl_2/{}^iPr_2NH$ (50 mL, 1:1 v/v). The purple solution was stirred overnight under inert atmosphere and refluxed. A redish-purple precipitate was formed, which was collected by filtration and washed with CH_2Cl_2 and dried under vacuum.

9. Yield: 63% (80.1 mg) ^1H NMR (MAS) (all bands are very large) δ (ppm): 9.07 (H-*meso*), 6.85 (H-*phenyl*), 4.50−2.01 (CH_2CH_3), 2.01-(−1.32) (CH_2CH_3). ^{31}P NMR (MAS) δ (ppm): 8.27. IR (KBr) ν: 2115.7 cm^{-1} (C≡C). Anal. Calcd (%) for $C_{88}H_{100}N_8P_2PtZn_2$ (1657.60): C 63.76, H 6.08, N 6.76. Found: C 63.87, H 6.33, N 6.87. MS (MALDI-TOF): m/z = 1657.63 $[M]^{+\bullet}$; 1657.60 calcd for $C_{88}H_{100}N_8P_2PtZn_2$. UV−visible (2MeTHF): λ_{max} nm ($\varepsilon \times 10^{-3}$, M^{-1} cm^{-1}) = 335 (26), 410 (121), 435 (52), 540 (24), 577 (24).

10. Yield: 46% (12.6 mg) ^1H NMR (MAS) (all bands are very large) δ (ppm): 9.57 (H-*meso*), 6.41 (H-*phenyl*), 4.48−1.71 (CH_2CH_3), 1.71-(−1.43) (CH_2CH_3). ^{31}P NMR (MAS) (ppm): 10.31. IR (KBr) ν: 2111.2 cm^{-1} (C≡C). Anal. Calcd (%) for $C_{88}H_{100}N_8P_2PtPd_2$ (1739.65): C 60.76, H 5.79, N 6.44. Found: C 60.75, H 5.92, N 6.11. MS (MALDI-TOF): m/z = 1738.47 $[M]^{+\bullet}$; 1739.65 calcd for $C_{88}H_{100}N_8P_2PtPd_2$.

11. Yield: 79% (23.1 mg) ^1H NMR (MAS) (all bands are very large) δ (ppm): 8.39 (H-*meso*), 6.55 (H-*phenyl*), 4.36−2.09 (CH_2CH_3), 2.09-(−1.94) (CH_2CH_3). ^{31}P NMR (MAS) δ (ppm): 6.74. IR (KBr) ν: 2111.2 cm^{-1} (C≡C). Anal. Calcd (%) for $C_{88}H_{100}N_8P_2PtPdZn$ (1698.63): C 62.22, H 5.93, N 6.60. Found: C 61.96, H 6.17, N 6.37. MS (MALDI-TOF): m/z = 1698.56 $[M]^{+\bullet}$; 1698.63 calcd for $C_{88}H_{100}N_8P_2PtPdZn$. UV−visible (2MeTHF): λ_{max} nm ($\varepsilon \times 10^{-3}$, M^{-1} cm^{-1}) = 335 (78), 412 (846), 515 (34), 547 (78), 576 (27).

Bis[5-*trans*-(4-ethynylphenyl)-13,17-diethyl-2,3,7,8,12,18-hexamethyl(metal)-porphyrin(bis(triethylphosphine)platinum(II)]-*trans*-5,15-bis(ethynylphenyl)-tetra-ethyl-2,8,12,18-tetramethyl-3,7,13,17-(zinc)porphyrin (metal = Zn (12), Pd (13)). CuI (~0.3 mg, ~0.0015 mmol) was added to a mixture of **5** (38.6 mg, 0.0360 mmol) or **6** (48.2 mg, 0.043 mmol) and [((HC≡$CC_6H_4)_2$(Zn(P))] (16.0 mg, 0.0220 mmol) in $CH_2Cl_2/{}^iPr_2NH$ (50 mL, 1:1 v/v). The purple solution was left to stir overnight under inert atmosphere and refluxed. A redish-purple precipitate was formed, which was collected by filtration, washed with CH_2Cl_2, and dried under vacuum.

12. Yield: 61% (24.8 mg) ^1H NMR (MAS) (all bands are very large) δ (ppm): 8.70 (H-*meso*), 7.09 (H-*phenyl*), 4.69−2.19 (CH_2CH_3), 2.19-(−1.80) (CH_2CH_3). ^{31}P NMR (MAS) δ (ppm): 5.50. IR (KBr) ν: 2109.5 cm^{-1} (C≡C). Anal. Calcd (%) for $C_{148}H_{172}N_{12}P_4Pt_2Zn_3$ (2829.31): C 62.83, H 6.13, N 5.94. Found: C 63.10, H 5.88, N 6.09. MS (MALDI-TOF): m/z = 2828.85 $[M]^{+\bullet}$; 2829.12 calcd for $C_{148}H_{172}N_{12}P_4Pt_2Zn_3$. UV−visible (2MeTHF): λ_{max} nm ($\varepsilon \times 10^{-3}$, M^{-1} cm^{-1}) = 340 (44), 413 (322), 540 (27), 575 (17).

13. Yield: 56% (35.1 mg) ^1H NMR (MAS) (all bands are very large) δ (ppm): 7.65 (H-*meso*), 6.23 (H-*phenyl*), 3.99−1.88 (CH_2CH_3), 1.88-(−1.01) (CH_2CH_3). ^{31}P NMR (MAS) δ (ppm): 10.97. IR (KBr) ν: 2098.1 cm^{-1} (C≡C). Anal. Calcd (%) for $C_{148}H_{172}N_{12}P_4Pt_2ZnPd_2$ (2911.36): C 61.06, H 5.95, N 5.77. Found: C 61.29, H 6.18, N 5.52. MS (MALDI-TOF): m/z= 2910.77 $[M]^{+\bullet}$; 2911.31 calcd for $C_{148}H_{172}N_{12}P_4Pt_2ZnPd_2$.

Instruments. ^1H NMR spectra for complexes **1**−**4** were recorded on a Bruker DRX-300 AVANCE spectrometer at the "Plateforme d'Analyse Chimique et de Synthèse Moléculaire de l'Université de Bourgogne (PACSMUB)". Chemical shifts are expressed in ppm relative to chloroform (7.258 ppm). The NMR spectra for complexes **5**−**8** were acquired on a Bruker AC-300 spectrometer (^1H 300.15 MHz and ^{31}P 121.50 MHz) using the solvent as a chemical shift standard, except for the ^{31}P NMR, where the chemical shifts are relative to D_3PO_4 85% in D_2O. All chemical shifts (δ) and coupling constants (J) are given in ppm and hertz, respectively. The spectra were measured from freshly prepared samples in chloroform. The NMR spectra for complexes **9**−**13** were characterized in the solid state. ^1H MAS NMR experiments (magic angle spinning) were performed at the National Ultrahigh-field NMR Facility for Solids (Ottawa, Canada) on a Bruker Avance II NMR spectrometer operating at 21.1 T. A double-resonance 3.2 mm Bruker probe. ^1H NMR chemical shifts were referenced to neat tetramethylsilane (TMS) using adamantane as a secondary chemical shift reference. ^1H MAS NMR spectra were recorded at a resonance frequency of 900.2 MHz. Samples were spun at a spinning speed of 20 kHz in 3.2 mm o.d. ZrO_2 rotors. A single pulse sequence with background suppression was used in the ^1H NMR experiments with the r.f. pulse length of 2.5 mks (pi/2 pulse) and a 10 s relaxation delay between pulses, which was found sufficient for a complete relaxation. A total of 64 scans were accumulated in each ^1H NMR experiment. The ^{31}P CP/MAS NMR spectra were acquired using a double-resonance 2.5 mm MAS Bruker probe at a resonance frequency of 364.4 MHz under 20 kHz MAS. The CP contact time in all experiments was 3 ms with a delay between acquisitions of 20 s. SPINAL-64 proton decoupling was used during spectra acquisition. From 256 to 2048 scans were collected depending on the amount of sample available. ^{31}P NMR chemical shifts were referenced to 85% H_3PO_4 using solid $(NH_4)H_2PO_4$ (ADP) as a secondary chemical shift reference. The same ADP sample was used to setup ^{31}P CP/MAS conditions. The mass spectra were obtained on a Bruker Daltonics Ultraflex II spectrometer at the PACSMUB in the MALDI/TOF reflectron mode using dithranol as a matrix. High resolution mass measurements (HR-MS) were carried out in the same conditions as previously using PEG ion series as internal calibrant or on a Bruker Micro-QTOF instrument in ESI mode. The infrared spectra were acquired on a Bomen FT-IR MB series spectrometer equipped with a baseline-diffused reflectance. The UV−visible spectra for compounds **1**−**4** were recorded on a Varian Cary 1 spectrophotometer. The UV−visible spectra for compounds **5**−**8** were recorded on a Hewlett-Packard diode array model 8452A. The emission spectra were obtained using a double monochromator Fluorolog 2 instrument from Spex. The emission lifetimes were measured on a TimeMaster Model TM-3/2003 apparatus from PTI. The source was nitrogen laser with high-resolution dye laser (fwhm ~1400 ps) and the fluorescence lifetimes were obtained from deconvolution or distribution lifetimes analysis. The uncertainties were about 50−100 ps. Some of the phosphorescence lifetimes were performed on a PTI LS-100 using a 1 μs tungsten-flash lamp (fwhm ~1 μs). The flash photolysis spectra and the transient lifetimes were

Scheme 2

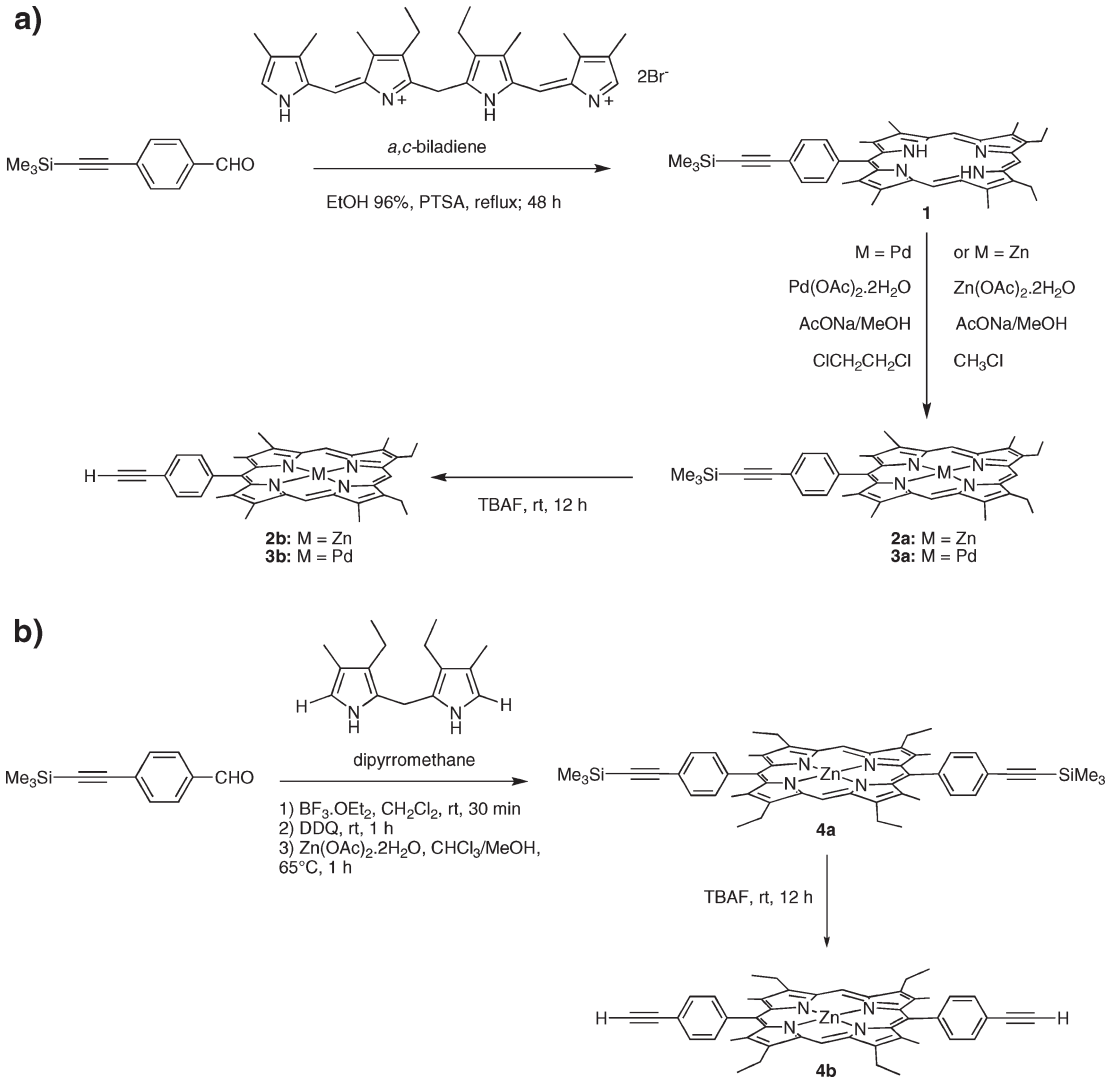

measured with a Luzchem spectrometer using the 355 nm line of a YAG laser from Continuum (Serulite), and the 530 nm line from OPO module pump by the same laser (fwhm = 13 ns).

Quantum yields measurements were performed in 2MeTHF at 77 and 298 K. Three different measurements (i.e., different solutions) were prepared for each photophysical datum (quantum yields and lifetimes). For the 298 K measurements, the samples were prepared under inert atmosphere (in a glovebox, $P_{O2} < 50$ ppm). For both temperatures, the sample and standard concentrations were adjusted to obtain an absorbance of 0.05 or less. This absorbance was adjusted to be the same as much as possible for the standard and the sample for a measurement. Each absorbance value was measured 10 times for better accuracy in the measurements of the quantum yields. The references used for quantum yields were Pd(TPP) (TPP = tetraphenylporphyrin; $\Phi = 0.14$)[42] for measuring porphyrin quantum yields and 9,10-diphenylanthracene ($\Phi = 1.0$)[43] for measuring the spacer quantum yields.

Results and Discussion

Syntheses and Characterization. There has been a tremendous amount of research devoted to the porphyrin syntheses with peripheral metal centers over the past few decades.[44] The porphyrins can be covalently linked to metal-containing centers by one or multiple carbon−metal bonds at the *meso* or β-positions of the porphyrin skeleton.[44] In search for new ways to interconnect porphyrins, platinum acetylide linkages have been previously used to synthesize conjugated organometallic porphyrin dimers, oligomers, or dendrimers.[45−53]

(42) Bolze, F.; Gros, C. P.; Harvey, P. D.; Guilard, R. *J. Porphyrins Phthalocyanines* **2001**, *5*, 569–574.
(43) Eaton, D. F. *Pure Appl. Chem.* **1988**, *60*, 1107–1114.
(44) Suijkerbuijk, B. M. J. M.; Klein Gebbink, R. J. M. *Angew. Chem., Int. Ed.* **2008**, *47*, 7396–7421.
(45) Chen, Y.-J.; Lo, S.-S.; Huang, T.-H.; Wu, C.-C.; Lee, G.-H.; Peng, S.-M.; Yeh, C.-Y. *Chem. Commun.* **2006**, 1015–1017.
(46) Ferri, A.; Polzonetti, G.; Licoccia, S.; Paolesse, R.; Favretto, D.; Traldi, P.; Russo, M. V. *J. Chem. Soc., Dalton Trans.* **1998**, 4063–4069.
(47) Harriman, A.; Hissler, M.; Trompette, O.; Ziessel, R. *J. Am. Chem. Soc.* **1999**, *121*, 2516–2525.
(48) Mackay, L. G.; Anderson, H. L.; Sanders, J. K. M. *J. Chem. Soc., Chem. Commun.* **1992**, 43–44.
(49) Monnereau, C.; Gomez, J.; Blart, E.; Odobel, F.; Wallin, S.; Fallberg, A.; Hammarström, L. *Inorg. Chem.* **2005**, *44*, 4806–4817.
(50) Onitsuka, K.; Kitajima, H.; Fujimoto, M.; Iuchi, A.; Takei, F.; Takahashi, S. *Chem. Commun.* **2002**, 2576–2577.
(51) Polzonetti, G.; Carravetta, V.; Iucci, G.; Ferri, A.; Paolucci, G.; Goldoni, A.; Parent, P.; Laffon, C.; Russo, M. V. *Chem. Phys.* **2004**, *296*, 87–100.
(52) Polzonetti, G.; Ferri, A.; Russo, M. V.; Iucci, G.; Licoccia, S.; Paolesse, R. *J. Vac. Sci. Technol. A* **1999**, *17*, 832–839.
(53) Yam, V. W.-W. *Acc. Chem. Res.* **2002**, *35*, 555–563.

Scheme 3

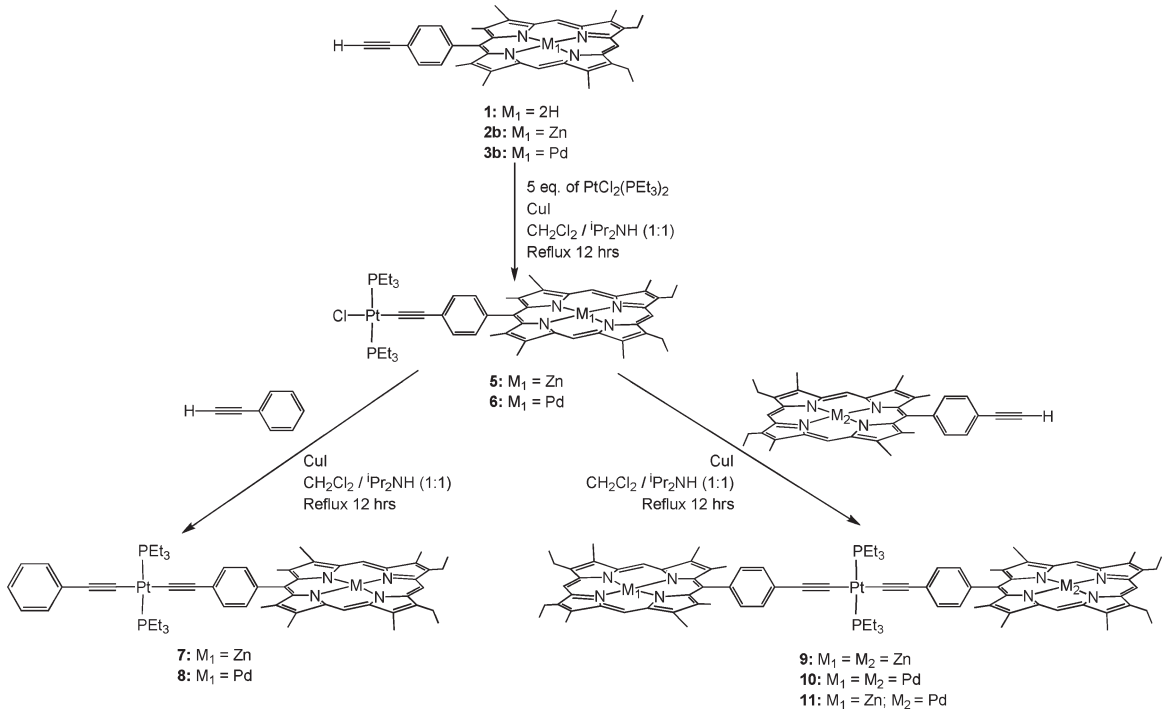

Scheme 4

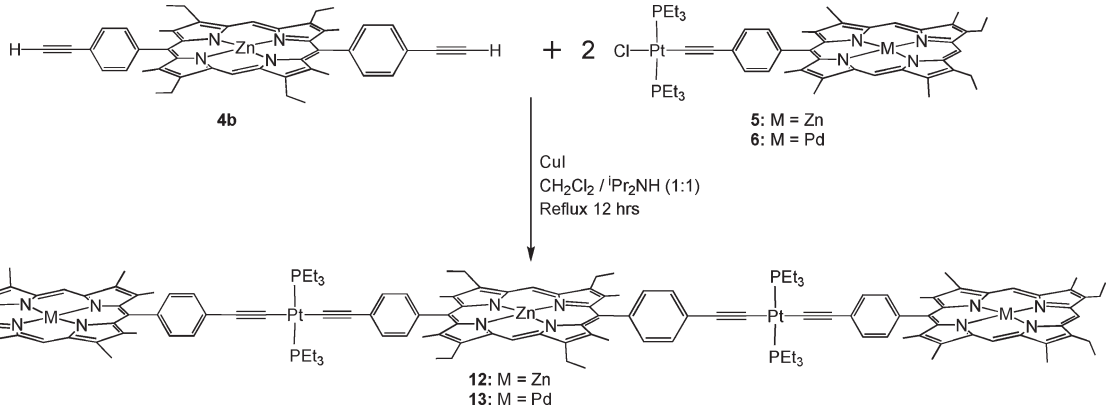

The synthetic routes leading to the target porphyrin-containing derivatives are outlined in Scheme 2a.

The condensation of 4-[2-(trimethylsilyl)ethynyl]benzaldehyde with the *a,c*-biladiene[38] afforded the expected free base porphyrin which can easily be metalated. The two metalation processes involve palladium acetate and zinc acetate yield the corresponding metalated porphyrins. The subsequent elimination of the trimethylsilyl group from the zinc- and palladium-containing porphyrins with NBu_4F in THF[54,55] produced the corresponding ethynyl porphyrins **2b** and **3b** in 78% and 96% yields, respectively. The resulting compounds were then used for the subsequent complexation with *trans*-dichlorobis(triethylphosphine)platinum(II)[39,40] to afford various monomers, dimers, and trimers below in good yields. The *trans*-substituted porphyrin building block **4a** was readily formed via a two-step one flask reaction of dipyrromethane and 4-[2-(trimethylsilyl)ethy;nyl]benzaldehyde at room temperature (Scheme 2b). The free-base was not isolated but in situ metal insertion allowed us to isolate the zinc complexes in 22% yield (not optimized). Desilylation of **4a** using NBu_4F at room temperature afforded the 5,15-diethynylporphyrin derivative **4b** in 93% yield.

The general procedure to synthesize monomeric, dimeric, and trimeric compounds **5**, **6**, **8**, **9**, **10**, **12**, and **13** involved a dehydrohalogenation reaction[56] between the *trans*-Pt-$(PEt_3)_2Cl_2$ and the appropriate ethynylporphyrin (**2b** or **3b**) in diisopropylamine in the presence of CuI (Schemes 3 and 4). The crude products **5**−**8** were purified via column chromatography (silica gel) using hexane/CH_2Cl_2 (40/60) as the solvents, and the products were isolated in 45−70% yields. Complexes **9**−**13** formed redish-purple precipitates, which were collected by filtration and washed with CH_2Cl_2.

(54) Nath, M.; Pink, M.; Zaleski, J. M. *J. Am. Chem. Soc.* **2005**, *127*, 478–479.

(55) Yen, W.-N.; Lo, S.-S.; Kuo, M.-C.; Mai, C.-L.; Lee, G.-H.; Peng, S.-M.; Yeh, C.-Y. *Org. Lett.* **2006**, *8*, 4239–4242.

(56) Sonogashira, K.; Fujikura, Y.; Yatake, T.; Toyoshima, N.; Takahashi, S.; Hagihara, N. *J. Organomet. Chem.* **1978**, *145*, 101–108.

Scheme 5

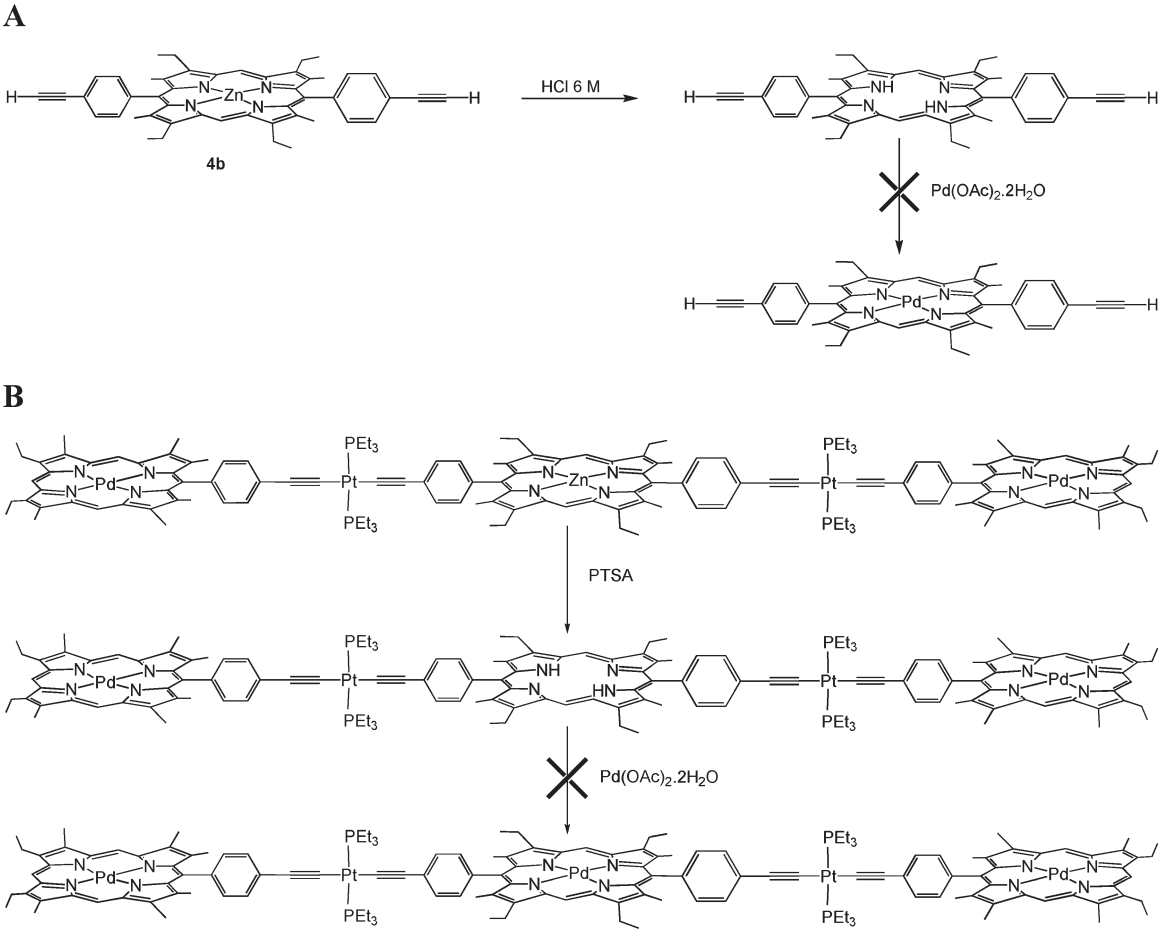

Attempts to prepare the homometallic trimer containing three palladium(II)-porphyrins was unfortunately unsuccessful. Two strategies were investigated. First, we attempted the demetalation of the starting bisethynylzinc(porphyrin). The demetalation step was readily performed using HCl (Scheme 5A). The following step was the coordination of palladium. A black insoluble precipitate was obtained but, unfortunately, it was concluded via spectroscopic comparison with the parent palladium-containing compounds **3b** and **10** that this precipitate was not the desired product. The second attempted route consisted of using compound **13** as the starting material followed by a demetalation process to remove the zinc. Unfortunately the zinc metal was not removed in the presence of HCl. Subsequently, a more soluble acid, the *para*-toluene sulfonic acid (PTSA), was used (Scheme 5B). The comparison of the UV−vis spectra confirmed that the zinc had been removed, hence forming the desired free base, and that the palladium metals remained in the peripheral porphyrin macrocycles. Subsequently, the addition of palladium (palladium acetate) was attempted. A soluble product was indeed obtained, but the comparison of the signature in the Q-region of the absorption spectra to compounds **12** and **13** did not resemble their spectral features. We then concluded that the desired product was unfortunately not obtained.

All the compounds were fully characterized by analytical and spectroscopic methods. The IR, NMR (^{1}H, and ^{31}P), and mass spectral data shown in the Experimental Section are consistent with their chemical structures. The IR spectra of these new metal complexes display a single sharp ν(C≡C) absorption band in the range of 2105−2120 cm^{-1}. The absence of the C≡C−H stretching mode of each compound around 3300 cm^{-1} indicates the formation of a C≡C—M bond. The NMR spectral data supports the conclusion that these compounds have well-defined and symmetric structures. The ^{31}P NMR spectra of compounds **5** and **6** exhibit a single resonance with a pair of Pt satellites, which is indicative of the *trans* geometry of the phosphine ligands about the platinum.

Spectroscopy and Photophysics. 1. Absorption Spectra. Absorption Spectra of the Parent PhC≡CPtL$_2$C≡CPh Compounds. The UV−vis spectra and MO descriptions (using density functional theory (DFT) and time-dependent DFT (TDDFT)) of the spacer and parent compounds of the type RC≡CPt(PR′$_3$)$_2$C≡CR (R = Ph; R′ = Et, Bu) were previously reported.[57−61] Only a brief account of the relevant information is provided here since this

(57) Emmert, L. A.; Choi, W.; Marshall, J. A.; Yang, J.; Meyer, L. A.; Brozik, J. A. *J. Phys, Chem. A* **2003**, *107*, 11340–11346.
(58) Wong, C.-H.; Che, C.-M.; Chan, M. C. W.; Han, J.; Leung, K.-H.; Philips, D. L.; Wong, K.-Y.; Zhu, N. *J. Am. Chem. Soc.* **2005**, *127*, 13997–14007.
(59) Batista, E. R.; Martin, R. L. *J. Phys. Chem. A* **2005**, *109*, 9856–9859.
(60) Cooper, T. M.; Krein, D. M.; Burke, A. R.; McLean, D. G.; Rogers, J. E.; Stagle, J. E. *J. Phys. Chem. A* **2006**, *110*, 13370–13378.
(61) Gagnon, K.; Aly, S. M.; Brisach-Wittmeyer, A.; Bellows, D.; Berube, J.-F.; Caron, L.; Abd-El-Aziz, A. S.; Fortin, D.; Harvey, P. D. *Organometallics* **2008**, *27*, 2201–2214.

Table 1. Absorption Spectral Data Measured in 2MeTHF at 298 K

	λ [nm]($\varepsilon \times 10^{-3}$ M^{-1} cm^{-1})		
compound	spacer	Soret band	Q bands
2b	332 (24)	410 (342)	540 (18) 575 (14)
3b	330 (19)	396 (237)	514 (20) 547 (51)
5	328 (27)	411 (302)	540 (18) 576 (11)
6	320 (32)	400 (265)	515 (22) 548 (53)
7	335 (26)	412 (210)	540 (10) 575 (6)
8	328 (40)	396 (211)	515 (17) 548 (43)
9	335 (26)	410 (121)	540 (52) 577 (24)
10[a]	335	400	515 549
11	335 (78)	412 (846)	515 (34)547 (78) 576 (27)
12	340 (44)	413 (322)	540 (27) 575 (17)
13[a]	340	400	420 515 548 580

[a] The solubility of these compounds in 2MeTHF was not sufficient enough for accurate absorptivity measurements.

fragment is used in the monomers, dimers, and trimers below. The complexes exhibit intense lowest energy absorption bands between 320 and 340 nm. For example, for R = Ph, these bands are found at 330 (shoulder; $\varepsilon = 43600$) and 337 nm ($\varepsilon = 44900$ M^{-1} cm^{-1}).[58] Earlier DFT calculations (B3LYP) for the PhC≡CPt$(PBu_3)_2$C≡CPh parent compound indicated that the highest occupied molecular orbital (HOMO) is composed of conjugated π-orbital of the PhC≡C unit along with a contribution from the Pt(d_{xy}) orbital. Concurrently, the lowest unoccupied molecular orbital (LUMO) consists of the ligand π^* orbital only.[57] Thus, the lowest energy excitation (i.e., HOMO → LUMO) for this Pt-containing spacer is a MLCT (metal-to-ligand-charge-transfer). This assignment is corroborated by the difference in band shape between the Pt complex (broad) and PhC≡CH ($\pi\pi^*$; narrow). Moreover, a more recent computational report (TDDFT) pointed out that this first excitation is in fact a mixture between two contributions, MLCT (59%) similar to that described above and LMCT (32%).[60] These two transitions arise from two different vertical but nearly degenerated excitations (difference only 0.04 eV; $\phi_g \rightarrow \phi_u^*$ and $\phi_u \rightarrow \phi_g^*$; where ϕ_g and ϕ_u and ϕ_g^* and ϕ_u^* are π- and π^*-orbitals, respectively, and with g orbitals including the Pt(d_{xy}) orbital).

Absorption Spectra of the Intermediates and the Spacer/Porphyrin Systems. Typical absorption spectra of the porphyrin-containing compounds include the intense Soret band (S_0-S_2 transition) and Q-bands (S_0-S_1 transition). The UV−visible data and absorptivities of the target monomeric, dimeric, and trimeric porphyrin derivatives and their synthesis intermediates are presented in Table 1.

For compounds **5**−**13**, the attachment of *trans*-C_6H_4C≡CPt$(PEt_3)_2$Cl or *trans*-C_6H_4C≡CPt$(PEt_3)_2$C≡CPh or *trans*-C_6H_4C≡CPt$(PEt_3)_2$C≡CC_6H_4- residues onto the porphyrin chromophores resulted in an intensity enhancement of the band in the UV-region (i.e., 300−350 nm) of the spectrum in comparison with the starting materials **2b** and **3b**. This new band is unambiguously characteristic of the spacer.

2. Emission Spectra. Emission Spectra of the Parent PhC≡CPtL_2C≡CPh Compounds. The *trans*-PhC≡CPt$(PBu_3)_2$C≡CPh compound exhibits a weak fluorescence band at room temperature in degassed 2MeTHF solutions, with a 0−0 peak localized at 346 nm and a quantum yield, Φ_F, < 0.0006.[57] Similarly, a weak fluorescence with a 0−0 peak at 356 nm was also detected for *trans*-(2,4,5-$Me_3C_6H_2$)C≡CPt$(PEt_3)_2$C≡C(2,4,5-$Me_3C_6H_2$) in degassed 2MeTHF at 298 K.[61] The fluorescence lifetime (τ_F) for this latter compound was < 0.1 ns, which is consistent with the weak quantum.[61]

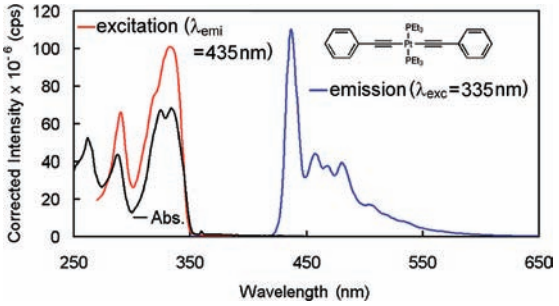

Figure 1. Emission (blue), excitation (red), and absorption (black) spectra of the parent compound *trans*-PhC≡CPt$(PEt_3)_2$C≡CPh in 2MeTHF at 77 K.

Moreover, compounds of the type *trans*-RC≡CPt$(PBu_3)_2$C≡CR (R = Ph, 2,4,5-$Me_3C_6H_2$, 2,4,6-$Me_3C_6H_2$) are strongly phosphorescent at 77 K (in 2MeTHF).[61] The phosphorescence bands exhibit a characteristic vibronic progression known for this class of compounds spreading from 440 to 600 nm with an intense 0−0 peak at ~450 nm.[57] A very weak fluorescence is occasionally observed, but its intensity is often too weak to allow the accurate measurements of τ_F and Φ_F. The strong phosphorescence coupled to the weak fluorescence is readily attributed to the heavy atom effect of the Pt metal. For comparison purposes, the emission spectrum of *trans*-PhC≡CPt$(PEt_3)_2$C≡CPh in 2MeTHF at 77 K is presented in Figure 1.

It was also occasionally noticed that when the fluorescence is more intense for some derivatives in comparison with the parent compounds *trans*-RC≡CPt$(PBu_3)_2$C≡CR, delayed fluorescence was present (see reference 61 for example). These luminescence features were readily detected from time-resolved spectroscopy in the μs time scale where both the phosphorescence and the fluorescence decays are the same (i.e., the fluorescence/phosphorescence intensity ratio is constant). We observed a similar feature here but this behavior was not investigated since this was not the purpose of this work.

Emission Spectra of the Synthesis Intermediates. The emission spectra and quantum yields for compounds **2b**−**6** in 2MeTHF are listed in Table 2 and are used for assignment purposes. The recorded spectra are given in the Supporting Information (Figure SI 1−4).

Emission Spectra of the Spacer/Porphyrin Systems. The emission spectra of the spacer-porphyrin monomers **7** and **8** (i.e., Zn(P)−C_6H_4C≡CPtL_2C≡CC_6H_5 and Pd(P)−C_6H_4C≡CPtL_2C≡CC_6H_5, respectively), the bridged porphyrin homobimetallic dimers Zn(P)−C_6H_4C≡CPtL_2C≡CC_6H_4−Zn(P), **9**, and Pd(P)−C_6H_4C≡CPtL_2C≡CC_6H_4−Pd(P), **10**, the heterobimetallic dyad Zn(P)−C_6H_4C≡CPtL_2C≡CC_6H_4−Pd(P), **11**, and the trimers Zn(P)−C_6H_4C≡CPtL_2C≡CC_6H_4−Zn(P)−C_6H_4C≡CPtL_2C≡CC_6H_4−Zn(P) (**12**) and Pd(P)−C_6H_4C≡CPtL_2C≡CC_6H_4−Zn(P)−C_6H_4C≡CPtL_2C≡CC_6H_4−Pd(P) (**13**) where L = PEt_3 were investigated in 2MeTHF at 77 and 298 K. The data are listed in Table 3.

Table 2. Luminescence Data for the Metalloporphyrin Chromophores **2b**−**6** in 2MeTHF

		λ (nm)				Φ[b]			
		77 K		298 K		77 K		298 K	
compound	lumophore[a]	fluorescence	phosphorescence	fluorescence	phosphorescence	Φ_F	Φ_P	Φ_F	Φ_P
2b	Zn(P)	575, 630	703, 785, 830 sh	597, 633		0.045	0.026	0.047	
3b	Pd(P)	545, 575, 597	662, 695, 717sh, 738	549, 600	668, 742sh	0.0016	0.40	0.0018	0.032
5	Zn(P)	576, 632	706, 788, 830 sh	580, 635		0.033	0.017	0.045	
6	Pd(P)	547, 598	664, 697, 719, 738	550, 600	670	0.0015	0.35	0.0017	0.0003

[a] Lumophores Zn(P) and Pd(P) are Zn(II) porphyrin and Pd(II) porphyrin, respectively. [b] The quantum yields are for the Zn(P) and Pd(P) chromophores only (λ_{exc} = 515 nm in all cases). The uncertainties in quantum yield values are ± 10% based on multiple measurements

Table 3. Luminescence Data Measured in 2MeTHF for **7**−**13**

		λ (nm)				Φ[b]			
		77 K		298 K		77 K		298 K	
compound	lumophore[a]	fluorescence	phosphorescence	fluorescence	phosphorescence	Φ_F	Φ_P	Φ_F	Φ_P
7	spacer		442, 463, 476, 490				0.042		
	Zn(P)	575, 632	705, 786, 835sh	580, 635		0.039	0.012	0.048	
8	spacer		442, 460, 477, 490sh				0.043		
	Pd(P)	547, 598	663, 697, 718sh	553, 607	673	0.0012	0.35	0.0014	0.0003
9	spacer		442				0.005		
	Zn(P)	575, 633	707, 788	581, 635		0.039	0.022	0.052	
10	spacer		440, 467, 490sh				0.005		
	Pd(P)	547, 598	663, 697, 718sh, 736	552, 608	668	0.0013	0.35	0.0016	0.002
11	spacer		445				0.004		
	Pd(P)	547	663	553	664sh	0.011[c]	0.094[c]	0.008[c]	
	Zn(P)	575, 633	706, 737sh, 786, 826sh	530, 635					
12	spacer		495				0.005		
	Zn(P)	576, 634	715, 798	580, 636		0.024	0.009	0.034	
13	spacer		495, 522				0.005		
	Pd(P)	546	664	552		0.0003[c]	0.092[c]	0.003[c]	
	Zn(P)	579, 636	698sh, 716, 737	587, 638					

[a] Zn(P) = Zn(II) porphyrin, Pd(P) = Pd(II) porphyrin, spacer = $C_6H_4C{\equiv}CPt(PEt_3)_2C{\equiv}CC_6H_4$. [b] The quantum yields are for the Zn(P) and Pd(P) chromophores only (λ_{exc} = 515 nm in all cases). The uncertainties in quantum yield values are ± 10% based on multiple measurements. [c] Because of the very strong overlap between the emission arising from the two chromophores, the total quantum yield is provided.

The emission spectra of the spacer-porphyrin monomers **7** and **8** in 2MeTHF at 77 K are presented in Figure 2; the corresponding spectra recorded at 298 K are given in the Supporting Information (Figure SI 5).

The emission spectra exhibit the signature of both the spacer and the porphyrin emissions. The phosphorescence originating from the $^3\pi\pi^*$ state of the spacer is readily identified in the 430−500 nm region with a 0−0 peak located at ~440 nm[58] (λ_{exc} = 350 nm). In comparison with the parent compounds *trans*-(2,4,5-$Me_3C_6H_2$)C≡CPt(PBu_3)$_2$C≡C-(2,4,5-$Me_3C_6H_2$) (Φ_P = 0.17)[61] and *trans*-(2,4,6-$Me_3C_6H_2$)C≡CPt(PBu_3)$_2$-C≡C(2,4,6-$Me_3C_6H_2$) (Φ_P = 0.38),[61] the relative intensity of the spacer phosphorescence is smaller for the spacer/porphyrin systems **7** and **8**. Indeed, the Φ_P's decrease to ~0.042 for both cases. This result indicates the presence of a supplementary non-radiative process in the spacer/porphyrin systems. Details for the spacer phosphorescence quantum yields are presented below.

On the other hand, the typical emissions of both the zinc(II)- and palladium(II)-porphyrins were also observed (λ_{exc} = 540 and 510 nm in the Q region, for convenience, for **7** and **8**, respectively). The $\pi\pi^*$ fluorescence of the metalloporphyrin chromophore was observed at 575 and 630 nm for **7** and at 547 and 597 nm for **8** as weak intensity bands. The weak intensity of the fluorescence of the Pd(P) chromophore in **8** is due to the heavy atom effect. Concomitantly, the intense emission bands are observed at 705 and 660 nm for **7** and **8**, respectively, and are assigned to the $\pi\pi^*$ phosphorescence of the metalloporphyrin chromophore.[42,62−65]

The emission spectra for the bridged porphyrin homobimetallic dimers Zn(P)−$C_6H_4C{\equiv}CPtL_2C{\equiv}CC_6H_4$−Zn-(P), **9**, and Pd(P)−$C_6H_4C{\equiv}CPtL_2C{\equiv}CC_6H_4$−Pd(P), **10** (L = PEt_3) in 2MeTHF at 77 K are shown in Figure 3. The corresponding spectra recorded at 298 K are given in the Supporting Information (Figure SI 6). While the spectra also exhibit the characteristic emission bands arising from the spacer and the porphyrins, the relative intensity of the spacer phosphorescence (λ_{exc} = 340 nm) versus that of the porphyrin emission is much smaller than that of the metalloporphyrin chromophores than what it would be anticipated for a ratio of 1:2 spacer versus metalloporphyrins. In fact, the Φ_P's decrease by another order of magnitude (~0.005). This result clearly reinforces the

(62) Harriman, A. *J. Chem. Soc., Faraday Trans. 2* **1981**, *77*, 1281–1291.
(63) Imahori, H.; Hagiwara, K.; Aoki, M.; Akiyama, T.; Taniguchi, S.; Okada, T.; Shirakawa, M.; Sakata, Y. *J. Am. Chem. Soc.* **1996**, *118*, 11771–11782.
(64) Pekkarinen, L.; Linschitz, H. *J. Am. Chem. Soc.* **1960**, *82*, 2407–2411.
(65) Sessler, J. L.; Jayawickramarajah, J.; Gouloumis, A.; Torres, T.; Guldi, D.; Maldonado, S.; Stevenson, K. J. *Chem. Commun.* **2005**, 1892–1894.

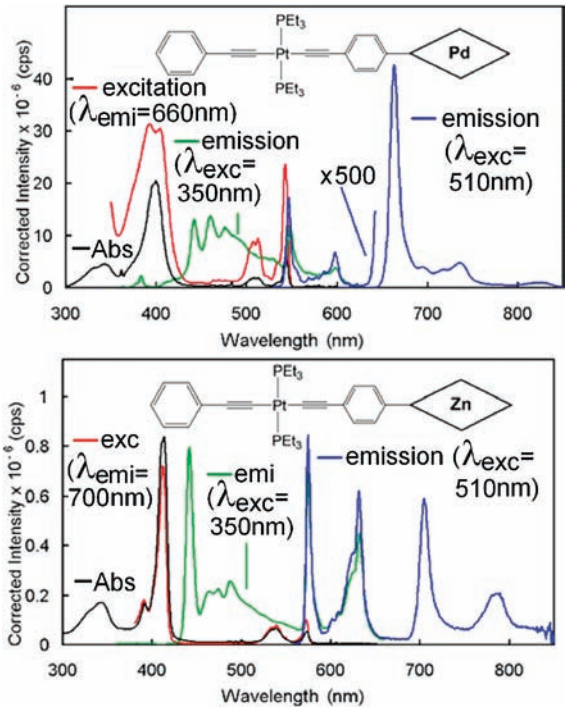

Figure 2. Emission (blue and green), excitation (red) and absorption (black) spectra of Zn(P)−$C_6H_4C{\equiv}CPtL_2C{\equiv}CC_6H_5$ (bottom, **7**) and Pd(P)−$C_6H_4C{\equiv}CPtL_2C{\equiv}CC_6H_5$ (top, **8**) in 2MeTHF at 77 K (L = PEt_3).

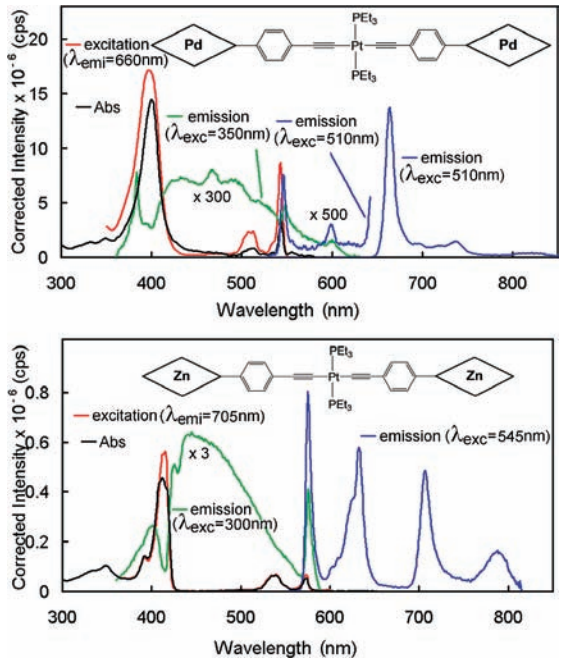

Figure 3. Emission (blue and green), excitation (red), and absorption (black) spectra of Zn(P)−$C_6H_4C{\equiv}CPtL_2C{\equiv}CC_6H_4$−Zn(P), **9** (bottom), and Pd(P)−$C_6H_4C{\equiv}CPtL_2C{\equiv}CC_6H_4$−Pd(P), **10** (top) in 2MeTHF at 77 K (L = PEt_3).

assumption that there is the presence of a non-radiative process efficiently deactivating the spacer excited states in the spacer/porphyrin systems.

The emission spectrum of the heterobismetallomacrocycle (Pd(P)−$C_6H_4C{\equiv}CPtL_2-C{\equiv}CC_6H_4$−Zn(P)), **11**,

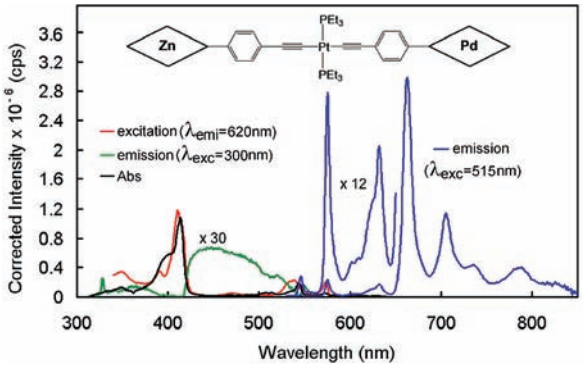

Figure 4. Emission (blue and green), excitation (red), and absorption (black) spectra of Pd(P)−$C_6H_4C{\equiv}CPtL_2C{\equiv}CC_6H_4$−Zn(P) (L = PEt_3) in 2MeTHF at 77 K.

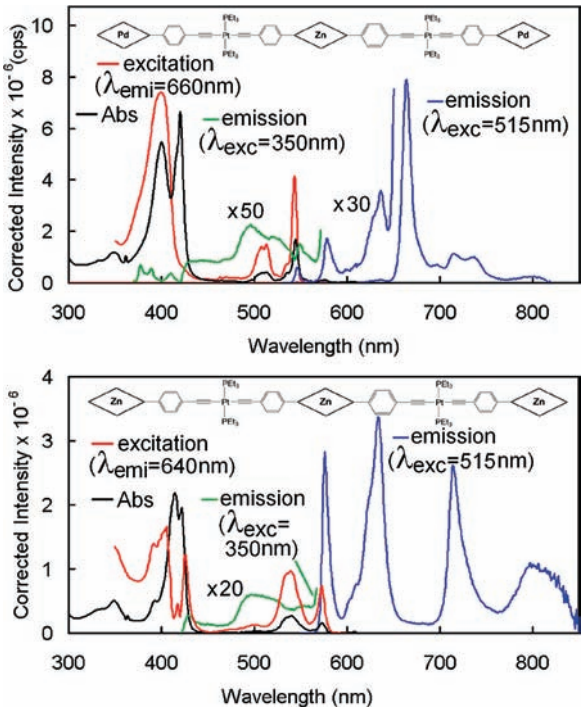

Figure 5. Emission (blue and green), excitation (red) and absorption (black) spectra of Zn(P)−$C_6H_4C{\equiv}CPtL_2C{\equiv}CC_6H_4$−Zn(P)−$C_6H_4$-$C{\equiv}CPtL_2C{\equiv}CC_6H_4$−Zn(P) ((L = PEt_3; bottom) and Pd(P)−C_6H_4-$C{\equiv}CPtL_2C{\equiv}CC_6H_4$−Zn(P)−$C_6H_4C{\equiv}CPtL_2C{\equiv}CC_6H_4$−Pd(P) (top) in 2MeTHF at 77 K.

in 2MeTHF at 77 K is given in Figure 4. The corresponding spectra recorded at 298 K are given in the Supporting Information (Figure SI 7). The characteristic emission bands arising from the spacer (in the 400−550 nm region; broad) and from both the palladium(II)- and the zinc(II)-porphyrins above 540 nm are readily observed. The Pd(P) fluorescence appears as a weak band at 545 nm, expected for this heavy metal-containing dyad, whereas that for the Zn(P) moieties is observed at 575 and 633 nm. A strong phosphorescence signal appears at 664 nm, which is readily attributed to the Pd(P) phosphorescence while the structured phosphorescence of the Zn(P) chromophore is observed in the 705−850 nm region. The Φ_P of the spacer (0.004) is weak as anticipated based on the observed data for **9** and **10** above.

Table 4. Emission Lifetimes for **2b**−**8** in 2MeTHF

	τ (λ_{emi} used; in nm)			
	77 K		298 K	
compound	fluorescence (ns)	phosphorescence	fluorescence (ns)	phosphorescence (μs)
2b	1.71 ± 0.03 (575)	27.8 ± 1.5 ms (780)	1.45 ± 0.06 (580)	
3b	0.17 ± 0.01 (545)	1810 ± 5 μs (663)	0.10 ± 0.03 (550)	97 ± 1 (665)
5	1.68 ± 0.04 (575)	24.1 ± 0.9 ms (780)	1.37 ± 0.02 (580)	
6	0.14 ± 0.01 (550)	1770 ± 10 μs (660) 90 ± 5 μs[a] (450)[a]	0.07 ± 0.02 (550)	b
7	1.66 ± 0.04 (575)	19.3 ± 0.1 ms (785)	0.88 ± 0.04 (575)	
8	0.16 ± 0.01 (550)	1740 ± 10 μs (660)	0.07 ± 0.01 (550)	b

[a] This emission is due to the phosphorescence of the $ClPt(PEt_3)_2C{\equiv}CC_6H_4$ chromophore. [b] Too weak to be measured accurately.

Table 5. Emission Lifetimes Measured in 2MeTHF

	τ (λ_{emi} used; in nm)			
	77 K		298 K	
compound	fluorescence (ns)	phosphorescence	fluorescence (ns)	phosphorescence (μs)
9	1.70 ± 0.02 (575)	23.3 ± 1.1 ms (780)	0.84 ± 0.02 (575)	
10	0.19 ± 0.01 (550)	1730 ± 20 μs (660)	0.09 ± 0.01 (550)	73.3 ± 3.4 (665)
11	1.69 ± 0.02 (575)	27.5 ± 0.7 ms (785)	0.73 ± 0.08 (580)	
	0.16 ± 0.02 (550)[a]	205 ± 20 μs (660) 69%	too weak (550)	
		1380 ± 50 μs (660) 31%		
12	1.44 ± 0.04 (575)	24.6 ± 1.2 ms (795)	0.89 ± 0.03 (580)	
13	1.43 ± 0.03 (575)	20.0 ± 0.4 ms (795)	0.79 ± 0.04 (575)	
	0.15 ± 0.01 (550)[a]	1680 ± 30 μs (660) 50%	0.08 ± 0.01 (550)	
		244 ± 33 μs (660) 50%		

[a] Examples of fast picosecond decays are provided in the Supporting Information (Figure SI 9).

Scheme 6

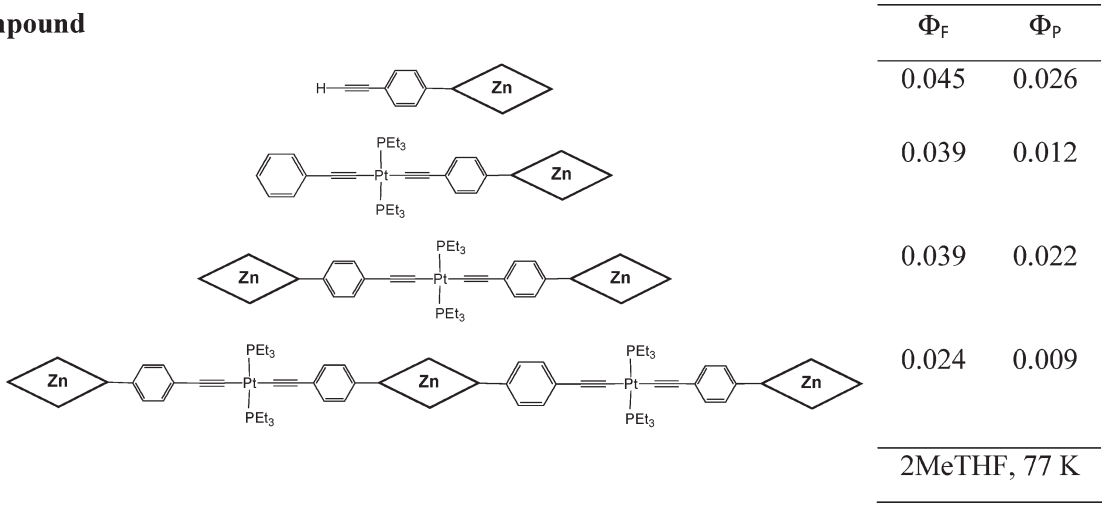

Similarly, the emission spectra of the trismetalloporphyrins $Zn(P)-C_6H_4C{\equiv}C-PtL_2C{\equiv}CC_6H_4-Zn(P)-C_6H_4C{\equiv}CPtL_2C{\equiv}CC_6H_4-Zn(P)$ (**12**) and $Pd(P)-C_6H_4C{\equiv}CPtL_2C{\equiv}C-C_6H_4-Zn(P)-C_6H_4C{\equiv}C-PtL_2C{\equiv}C-C_6H_4-Pd(P)$ (**13**) also exhibit the characteristic emissions of both the spacers and porphyrin macrocycles (Figure 5). The corresponding spectra recorded at 298 K are given in the Supporting Information (Figure SI 8). Unsurprisingly, the Φ_P for the spacer phosphorescence is low (0.005) as for compounds **9**, **10**, and **11**. The spectral and Φ_P data for the studied compounds in 2MeTHF are listed in Table 3.

The Φ_e data (Φ_F and Φ_P) for the metalloporphyrin chromophores also undergo changes with the structure. Scheme 6 shows a representative example of the effect of the structure on the Φ_e data. Going from **2b** → **7** → **9** → **12** in 2MeTHF at 77 K, Φ_F should increase with the number of Zn(P) chromophores in the molecule, but in overall, it decreases. This observation is consistent with the heavy metal effect induced by the Pt atoms. On the other hand, Φ_P should increase in the same order, but in overall, it decreases with some fluctuation. The increase in the number of chromophores should induce an increase in Φ_P as well observed going from **7** to **9**, but the introduction of the PEt_3 ligand also introduces a loose-bolt effect

Chart 2

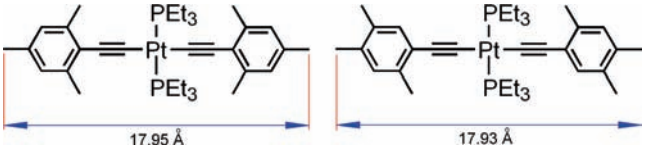

(decreasing radiative processes to the profit of non-radiative)[66] as well observed going from **2b** to **7** (by a factor of ~2) and from **9** to **12** (also by a factor of ~2).

3. Emission Lifetimes and S_1 and T_1 Energy Transfers (λ_{exc} is in the Q-bands). Emission Lifetimes of the Ligands and Intermediates. The emission lifetimes of the ligands and intermediates (**2b**−**6**) measured in 2MeTHF are given in Table 4. These data are used for comparison and assignment purposes in the spacer/metalloporphyrin systems. They appear typical in comparison with other emission lifetimes and are not discussed further.[67] In a qualitative manner, the trend observed for Φ_F and Φ_P (see Scheme 6 for example) follows that of the corresponding emission lifetimes.

Emission Lifetimes and Pd(P) → Zn(P) S_1 and T_1 Energy Transfers in the Spacer/Porphyrin Systems 9−**13.** On the basis of the position of the 0−0 peaks of the fluorescence and phosphorescence of the comparison molecules **2b**−**8**, the Pd(P) and Zn(P) chromophores are readily assigned as the S_1 and T_1 energy donor and acceptor, respectively. A close comparison of τ_F at 298 and 77 K of the Zn(P) chromophore going from **9** to **11** (Table 5), shows a small decrease (excluding the uncertainties) consistent with the heavy metal effect (as one Zn atom is replaced by one Pd). This is interesting because this subtle "information" is passed across the spacer (~18 Å),[61] suggesting communication. The comparison of τ_F of the Pd(P) chromophore going from **10** (for which no energy transfer takes place; donor-spacer-donor) to **11** also indicates a decrease (also excluding the uncertainties). In the absence of energy transfer, one would expect that τ_F(Pd(P)) would be larger for **11** (since it has only one Pd atom). This is obviously not the case and this information suggests S_1 energy transfer. Indeed, we have previously reported an exhaustive study on S_1 through space energy transfer in cofacial bisheteromacrocycles (M = Zn, M′ = Pd).[68,69] But a clear evidence for energy transfer comes from the comparison of τ_P(Pd(P)) between **10** and **11**, and between **10** and **13**. Compound **10** is used as a comparison molecule for the trimer as well because the synthesis of the trispalladium(II) porphyrin analogue was unsuccessful (see above).

Prior to discussing further the energy transfer processes, a look at the τ_P data for **11** and **13** is necessary. Both compounds exhibit decays with two components (i.e., $2\tau_P$(Pd(P))). The similarity of the long components (1380 ± 50 μs for **11** and 1680 ± 30 μs for **13**) with that for

Chart 3

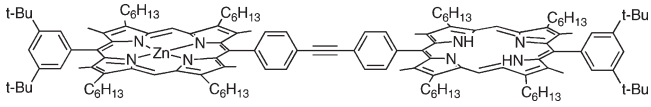

10 (1730 ± 20 μs) suggests very slow T_1 energy transfer (Pd(P) → Zn(P)). On the other hand, the fast components (205 ± 20 μs for **11** and 244 ± 33 μs for **13**) suggest faster transfer. To explain these components, one may consider the X-ray structures of the related compounds *trans*-RC≡CPt(PBu_3)$_2$C≡CR (Chart 2; R = 2,4,6-$Me_3C_6H_2$, 2,4,5-$Me_3C_6H_2$).[61]

Indeed, the angle formed by the aryl and $PtP_2(C{\equiv}C)_2$ planes are 83 and 30°, respectively. These orientations cannot exhibit the same electronic communication via conjugation (across the d orbital of the Pt center). If T_1 energy transfer operates dominantly via a Dexter mechanism (double electron exchange),[69] then orbital overlap is clearly important in conjugated systems. The existence of two (or more) rotamers in solution would hypothetically lead to different photophysical responses in energy transfers.

If there are two components for the τ_P decays for **11** and **13**, then we should logically get two as well for the τ_F decays. The easiest component to measure is the slow one (here 0.16 ± 0.02 for **11** and 0.15 ± 0.01 ns for **13**), then the faster one should proportionally be 1 order of magnitude smaller as well. If this is the case, then the predicted components should be measured in the 0.020−0.010 ns time scale, which is within the uncertainty of the method.

The rates for both the S_1 and T_1 energy transfers can be calculated using eq 1:[67]

$$k_{ET} = \left(\frac{1}{\tau_e} - \frac{1}{\tau_e^0}\right) \quad (1)$$

where, τ_e^0 is the emission lifetime for a comparative donor−donor system where no energy transfer takes place, and τ_e is the emission lifetime of the donor in the dyad. The donor−donor and donor−acceptor systems are **10** and **11**, respectively. For **13**, the tris-palladium analogue is not available. The rates for singlet and triplet energy transfers, $k_{ET}(S_1)$ and $k_{ET}(T_1)$ are ~2×10^9 s^{-1} and 0.15×10^3 (slow component) and 4.3×10^3 s^{-1} (fast component), respectively. The uncertainty on $k_{ET}(S_1)$ is obviously large, but this value compares very favorably to that reported by Osuka and collaborators ($k_{ET}(S_1) = 2.3 \times 10^9$ s^{-1}) in a dyad closely related to compound **11** (Chart 3; Zn(P) and H_2(P) are the energy donor and acceptor, respectively).[70] The presence of methyl groups at the β-position provides the appropriate aryl-porphyrin chemical environment for acceptable comparison.

On the other hand, the $k_{ET}(T_1)$ values fall short by 1 or 2 orders of magnitude in comparison with structurally related dyads reported by Albinsson and collaborators (Chart 4).[71] This comparison indicates that the replacement of the aryl group in the Albinsson series by Pt slows

(66) Turro, N. J. *Modern Molecular Photochemistry*; Benjamin/Cummings Pub. Co.: Menlo Park, CA, 1978.
(67) Harvey, P. D. In *The Porphyrin Handbook*; Kadish, K. M., Smith, K. M., Guilard, R., Eds.; Academic Press: San Diego, CA, 2003; Vol. *18*, pp 63−250.
(68) Faure, S.; Stern, C.; Guilard, R.; Harvey, P. D. *J. Am. Chem. Soc.* **2004**, *126*, 1253–1261.
(69) Faure, S.; Stern, C.; Espinosa, E.; Guilard, R.; Harvey, P. D. *Chem.—Eur. J.* **2005**, *11*, 3469–3481.
(70) Osuka, A.; Tanabe, N.; Kawabata, S.; Yamazaki, I.; Nishimura, Y. *J. Org. Chem.* **1995**, *60*, 7177–7185.
(71) Jensen, K. K.; van Berlekom, S. B.; Kajanus, J.; Martensson, J.; Albinsson, B. *J. Phys. Chem. A* **1997**, *101*, 2218–2220.

Chart 4

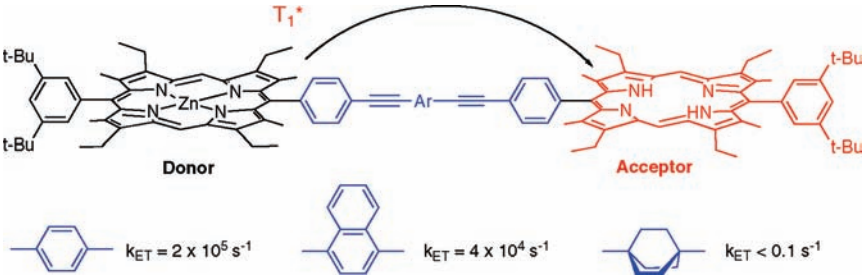

Table 6. Emission Lifetimes of the *trans*-$C_6H_4C{\equiv}CPt(PEt_3)_2C{\equiv}CC_6H_4$ Spacers and T_1 Energy Transfer Rates for Spacer → M(P) (M = Zn, Pd).[a]

compound	τ_P (monitored at λ_{emi} nm)	k_{ET} (T_1) (s^{-1})
7	36.2 ± 0.4 μs (440)	1.6×10^4
8	31.1 ± 2.8 μs (460)	2.0×10^4
9	24.1 ± 3.6 μs (460)	3.0×10^4
10	24.7 ± 2.6 μs (460)	2.9×10^4
11	20.0 ± 2.7 μs (460)	3.8×10^4
12	weak signal	b
13	weak signal	b

[a] In 2MeTHF at 77K. [b] Too weak to be accurately measured.

down the rates of transfer. The comparison with the spacer containing a saturated fragment illustrates the effect of poor conjugation on $k_{ET}(T_1)$.

Because the fluorescence and phosphorescence lifetimes of compounds **12** and **13** resemble that of **10** and **11**, the k_{ET} values are expected to be in the same range, but their accurate evaluations are not possible.

Emission Lifetimes When Excited in the Spacer Absorption Band (around 320 nm) and Triplet Energy Transfer. (a). Emission Lifetimes of the *trans*-PhC≡CPtL$_2$C≡CPh Spacer and Related Derivatives. For the compounds of the type *trans*-RC≡CPt$(PEt_3)_2$C≡CR with R = 2,4,5-$Me_3C_6H_2$, 2,4,6-$Me_3C_6H_2$, Ph, the τ_P's are 85, 50, and 35.0 ± 1.3 μs, respectively.[61] This trend follows the number of methyl groups located at the *ortho*-positions (τ_P varies as 2 > 1 > 0), and may reflect the relative ease for the aryl groups to rotate about the Pt−C≡C−Ar axis. This motion, if present, may contribute to the non-radiative relaxation to the ground state. This feature is important since the spacers used in this work do not exhibit Me groups at the *ortho*-position. However, the rotation is prevented by the presence of methyl groups placed at the β-positions of the metalloporphyrin macrocycle. Indeed, for compound **6** we find $\tau_P = 90 \pm 5$ μs. Therefore, the compound exhibiting 85 μs is more suitable for calculating k_{ET}'s below.

(b). Phosphorescence Lifetimes of the *trans*-C_6H_4-C≡CPtL$_2$C≡CC_6H_4 Spacer in Compounds 7−13. The spacer τ_P's for **7**−**11** are listed in Table 6. They are in the same range as the parent compounds *trans*-RC≡CPt$(PEt_3)_2$C≡CR with R = 2,4,5-$Me_3C_6H_2$, 2,4,6-$Me_3C_6H_2$, Ph discussed above, but quenching is obvious. The "loose bolt" effect on the emission lifetime is negligible as the macrocycles are rigid components (in comparison with the more flexible PEt_3 ligands).[66]

The emission lifetimes listed in Table 6 can be separated into 3 groups: the monomers **7** and **8**, dimers **9**−**11**, and trimers **12** and **13**. The lifetimes decrease going from monomers to dimers, and the intensity becomes too weak

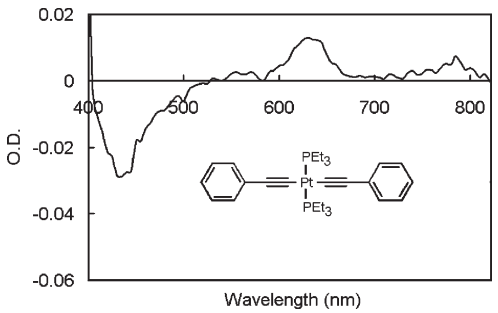

Figure 6. Transient absorption spectrum of *trans*-PhC≡CPt$(PEt_3)_2$C≡CPh in 2MeTHF at 77 K (λ_{exc} = 355 nm, delay = 0.1 μs). The negative signal at 430 nm is due to phosphorescence.

(and most likely short as well) for accurate measurements in the trimers. This behavior is assigned to a T_1 energy transfer (spacer → M(P); M = Zn, Pd) and using eq 1 the k_{ET} values are extracted (Table 6). The data are in the 10^4 s^{-1} range, a range that compares favorably to that reported by Albinsson and collaborators for structurally related dyads.[71] These values are also faster than that for the T_1 Pd(P)* → Zn(P) transfer in compound **11**, again demonstrating clearly that the bond between the *meso*-C and the aryl group does not slow down the T_1 transfer but rather the Pt metal does. The demonstration that T_1 energy transfer is the sole process (i.e., no electron transfer) is provided by transient absorption spectroscopy in the nanosecond time scale.

Transient Absorption Spectra and Lifetimes (λ_{exc} = 355 nm). (a). PhC≡CPtL$_2$C≡CPh Parent Compounds. For the PhC≡CPt$(PBu_3)_2$C≡CPh compound, the triplet excited state dynamics can still be accessible from T_1-T_n absorptions. The reported T_1-T_n band is located in the 400−700 nm window placed at ~645 nm. The transient lifetime is 590 ± 150 ps.[72] To increase the lifetime of the transient species, investigations at 77 K using a Dewar assembly can be performed. We measured the transient absorption spectrum of *trans*-PhC≡CPt$(PEt_3)_2$C≡CPh (Figure 6). A narrow T_1-T_n absorption band is observed at ~620 nm, which is in agreement with that reported for *trans*-PhC≡CPt$(PBu_3)_2$C≡CPh. The transient lifetime is 36 μs and compares favorably to that of the phosphorescence lifetime (35.8 μs) confirming the assignment.

(72) (a) de Santana, H.; Quillard, S.; Fayad, E.; Louarn, G. *Synth. Methods* **2006**, *156*, 81–85. (b) Han, C.-C.; Balakumar, R.; Thirumalai, D.; Chung, M.-T. *Org. Biomol. Chem.* **2006**, *4*, 3511–3516. (c) Nishiumi, T.; Chimoto, Y.; Hagiwara, Y.; Higuchi, M.; Yamamoto, K. *Macromolecules* **2004**, *37*, 2661–2664. (d) Nishiumi, T.; Nomura, Y.; Chimoto, Y.; Higuchi, M.; Yamamoto, K. *J. Phys. Chem. B* **2004**, *108*, 7992–8000. (e) Temme, O.; Laschat, S.; Frohlich, R.; Wibbeling, B.; Heinze, J.; Hauser, P. *J. Chem. Soc., Perkin Trans. 2* **1997**, 2083–2085.

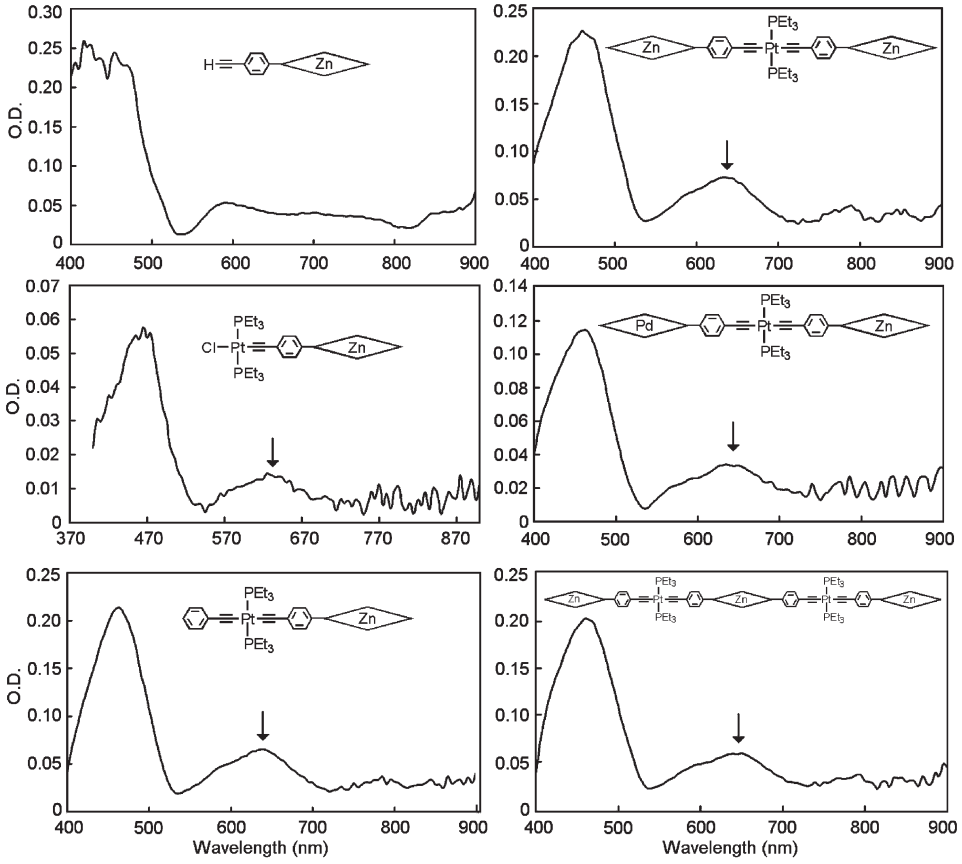

Figure 7. Transient absorption spectra of **2b** (up left), **5** (middle left), **7** (bottom left), **9** (up right), **11** (middle right), and **12** (bottom right) in 2MeTHF at 298 K (λ_{exc} = using 355 nm; delay = 0.1 μs). The arrow indicates the absorption band for $Zn(P)^+$.

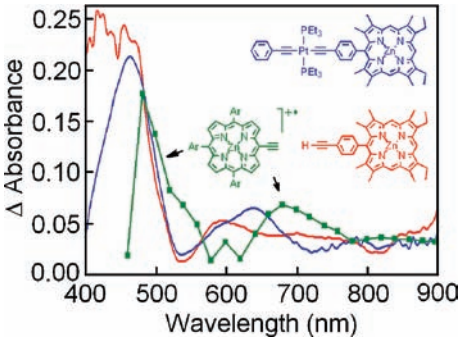

Figure 8. Comparison of the transient absorption spectra of **2b** (red), **7** (blue) in 2MeTHF at 298 K (λ_{exc} = using 355 nm; delay = 0.1 μs) and the dyad presented in Chart 5 (green; Ar = 3,5-$(t$-Bu$)_2C_6H_3$). The green spectrum is redrawn and modified from reference. [73]

(b). Transient Absorption Spectra and Lifetimes of the Synthesis Intermediates 2b−13. The transient absorption spectra for Zn(P)−containing compounds, **2b**, **5**, **7**, **9**, **11**, **12**, and **13**, in 2MeTHF at 298 K (Figure 7) exhibit two distinctive features. The first one is a strong absorption characteristic of the porphyrin macrocycle at ~470 nm as well exemplified by the spectrum of compound **2b**. This feature is accompanied by a "valley" located at ~535 nm resembling a bleach of a Q-band.

The second feature is the presence of a broad band at ~640 nm for this series except **2b**. This broad feature falls close to the transient T_1-T_n absorption at ~620 nm for the

Chart 5. [a]

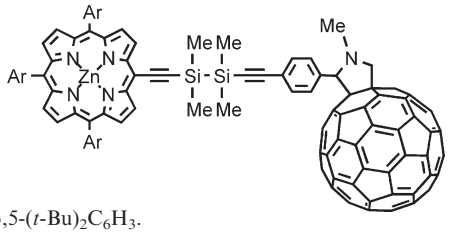

[a] Ar = 3,5-$(t$-Bu$)_2C_6H_3$.

trans-PhC≡CPt$(PEt_3)_2$C≡CPh parent compound. However the broadness of this signal and its absence from the spectra of the Pd(P)−containing analogues (the spectra are provided in the Supporting Information; Figure SI 10) suggest that this feature may not be the T_1-T_n absorption of the Pt-containing spacer.

The possibility of electron transfer was also considered. The $Zn(P)^+$ cation generated by a photoinduced electron transfer in a dyad formed of a Zn(P) chromophore and the strong electron acceptor C_{60} (Chart 5) was recently investigated.[73] Figure 8 compares the transient absorption spectra of **2b** (red), **7** (blue), and the Zn(P)−C_{60} dyad presented in Chart 5 (green; Ar = 3,5-$(t$-Bu$)_2C_6H_3$).[73] The latter dyad exhibits a signal centered at about 700 nm for the corresponding $Zn(P)^+$ chromophore, which is significantly different from the T_1-T_n signal of the Pt-containing spacer located at

(73) Tsuji, H.; Sasaki, M.; Shibano, Y.; Toganoh, M.; Kataoka, T.; Araki, Y.; Tamao, K.; Ito, O. *Bull. Chem. Soc. Jpn.* **2006**, *79*, 1338–1346.

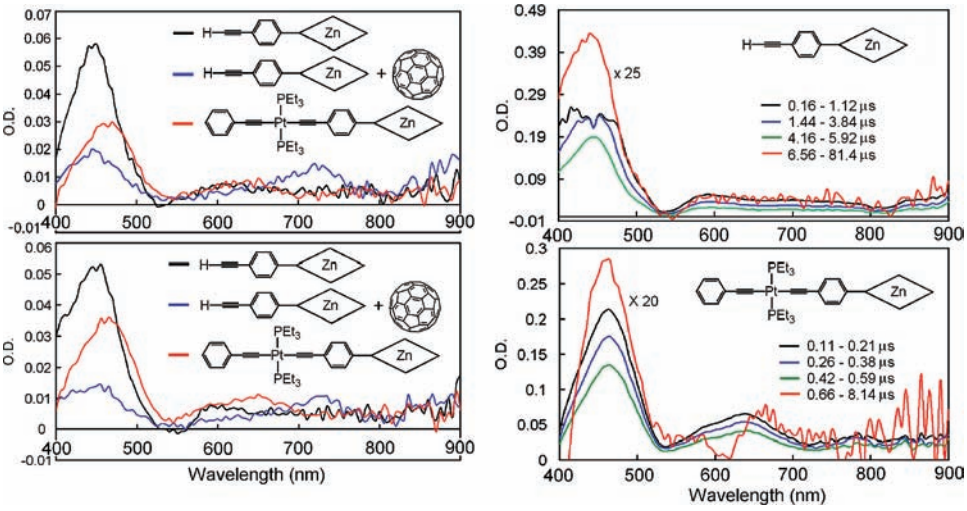

Figure 9. Left: Transient absorption spectra of **2b** (black), **2b** + C_{60} (blue), and **7** (red) in benzene (up) and ethanol (down). $\lambda_{exc} = 355$ nm; delay = 0.1 μs. Right: Time-resolved transient absorption spectra of **2b** (up) and **7** (down) in 2MeTHF at 298 K; $\lambda_{exc} = 355$ nm.

~640 nm. So this ~640 nm feature cannot be assigned to the equivalent $Zn(P)^+$.

Moreover, the second product of this photoinduced electron transfer is the radical anion [*trans*-C_6H_4-$C{\equiv}CPtL_2C{\equiv}CC_6H_4$]. On the basis of the literature,[74] the transient absorption spectrum exhibits a low-energy feature between 1000 and 1400 nm, a range that is not accessible on our instrument. It also exhibits a higher energy band at 540 nm, but in our spectra this position falls at a place where a bleach of a Q-band takes place. This is particularly true for the Pd(P)-containing compounds where the bleach is more pronounced (i.e., exhibiting a negative signal; Supporting Information, Figure SI 10).

In an attempt to address the nature of this band, other tests were performed. Figure 9 exhibits the transient absorption spectra of compound **2b** in the presence and in the absence of C_{60} using benzene and ethanol as the solvents. In the presence of C_{60}, quenching of the triplet excited state is observed from the decrease of the signal at 450 nm for identical concentrations and delay times. Moreover, a new transient feature is observed at ~720 nm. This band is readily assigned to the corresponding $Zn(P)^+$ cation[75] and is clearly absent from the transient absorption spectra of **7** (Figure 9).

The time-resolved transient spectra show no evidence for two different species as clearly seen in Figure 9 on the right-hand side. So species arising from a photoinduced electron transfer can be ruled out, and the transient spectra are dominated by the T_1-T_n signature of the M(P) chromophores (M = Zn, Pd). The photophysical events in this time scale (> 13 ns) are only T_1 energy transfers.

Conclusion

A series of linear monomers (spacer−M(P)), dimers (M(P)−spacer−M′(P)), and trimers (M(P)−spacer−M′-(P)−spacer−M(P)) of spacer/metalloporphyrin systems, including mixed metalloporphyrin compounds, where the spacer is the rigid and conjugated Pt-containing *trans*-$C_6H_4C{\equiv}CPtL_2C{\equiv}CC_6H_4$- fragment were synthesized and characterized. Both the spacer and the metalloporphyrin macrocycle are luminescent allowing the monitoring of the photophysical proerties as a function of structural changes. The excitation in the Q-bands of the Pd(P) chromophores leads to S_1 and T_1 energy transfers to the Zn(P) units (i.e., Pd(P)*→Zn(P)). The rates are found modest (~2×10^9 s^{-1}, S_1, and 0.15×10^3 (first component) and 4.3×10^3 s^{-1} (second component), T_1), which is consistent with the presence of the spacer, a spacer where the conformation is limited to a quasi-perpendicular orientation of the aryl and porphyrin planes (because of the presence of two β-methyl groups). Importantly, it is concluded that the Pt atom slows down the transfer when comparing to related dyads that do not contain a Pt-atom in the conjugated chain. The excitation in the absorption band of the *trans*-C_6H_4-$C{\equiv}CPtL_2C{\equiv}CC_6H_4$- spacer in the 300−360 nm range also leads to T_1 energy transfer (spacer* → M(P); M = Zn, Pd) and a decrease in the phosphorescence intensity is observed. The rates for T_1 energy transfer measured by the change in phosphorescence lifetimes are in the 10^4 s^{-1} range. This time scale lies on the slow side of the list of rates known for porphyrin-containing molecules.[67] This time frame (10^4 s^{-1}) is faster than that for the T_1 Pd(P)*→Zn(P) transfers above (10^3 s^{-1}), hence corroborating that the spacer-metalloporphyrin single bond located on *meso*-C atom is not the major barrier slowing down the transfer (but rather the Pt atom in this case).

These non-radiative processes (S_1 and T_1 energy transfers) in these monodisperse oligomers bear direct relevance to the corresponding metalloporphyrin-containing polymers, (−spacer−M(P)−)$_n$, as potential materials for photonic applications (i.e., solar cells).

Finally, this work stresses the interesting resemblance between the LH II system (for example) in the purple photosynthetic bacteria discussed in the Introduction. Among the phenomena, the energy transfer process S_1 B800* → B850 which is very fast (~1.2 ps time scale) despite the long center-to-center separation (~18 Å) was suspected to use the carotenoid as relay. This work demonstrates that this

(74) Cardolaccia, T.; Funston, A. M.; Kose, M. E.; Keller, J. M.; Miller, J. R.; Schanze, K. S. *J. Phys. Chem. B* **2007**, *111*, 10871–10880.
(75) Losev, A. P.; Bachilo, S. M.; Volkovich, D. I.; Avlasevich, Y. S.; Solov'yov, K. N. *J. Appl. Spectrosc.* **1997**, *64*, 62–71.

phenomenon is indeed possible since S_1 energy transfer (Pd(P)* → Zn(P)) is possible with a relatively good rate (~100 ps time scale). The difference in rates for this comparison is due to the larger change in dipole moment of the bacteriochlorophyll *a* chromophore in comparison with the symmetric metalloporphyrin unit. This choice was based on synthetic convenience.

The presence of Pt in the spacer allowed monitoring the rates of transfer in the T_1 states. The slow rates observed remind us that nature elected not to use the T_1 energy transfer as a pathway for energy migration. Indeed, one of the roles of the carotenoid is to quench the T_1 state in LH II if populated. In addition, the excitation in the absorption band of the organometallic spacer here allowed us to observe. A study of the chain length dependence on the photophysical properties of longer oligomers is in progress and will be published in due course.

Acknowledgment. This research was supported by the Natural Sciences and Engineering Research Council of Canada (NSERC), *le Fonds Québécois de la Recherche sur la Nature et les Technologies* (FQRNT), and the Centre d'Études des Matériaux Optiques et Photoniques de l'Université de Sherbrooke. The authors thank Dr. Victor V. Terkikh for the NMR measurements with access to the 900 MHz NMR spectrometer which was provided by the National Ultrahigh Field NMR Facility for Solids (Ottawa, Canada), a national research facility funded by the Canada Foundation for Innovation, the Ontario Innovation Trust, Research Quebec, the National Research Council Canada, and Bruker Biospin and managed by the University of Ottawa (www.nmr900.ca). The Natural Sciences and Engineering Research Council of Canada (NSERC) is acknowledged for a Major Resources Support grant. The French Ministry of Research (MENRT), CNRS (UMR 5260) is also gratefully acknowledged. The authors are also grateful to M. Albini for the synthesis of pyrrole and dipyrromethane precursors.

Supporting Information Available: Emission, excitation and absorption spectra in 2MeTHF at 77 and 298 K of starting material Zn(P)−$C_6H_4C{\equiv}CH$ (**2b**) and Pd(P)−$C_6H_4C{\equiv}CH$ (**3b**) (Figure SI 1 and SI 2); and intermediates Zn(P)−$C_6H_4C{\equiv}CPtL_2Cl$ (**5**) and Pd(P)−$C_6H_4C{\equiv}CPtL_2Cl$ (**6**) (Figure SI 3 and SI 4). Emission, excitation and absorption spectra of Zn(P)−$C_6H_4C{\equiv}CPtL_2C{\equiv}CC_6H_6$ (**7**), Pd(P)−$C_6H_4C{\equiv}CPtL_2C{\equiv}CC_6H_6$ (**8**) (Figure SI 5), Zn(P)−$C_6H_4C{\equiv}CPtL_2C{\equiv}CC_6H_4$−Zn(P) (**9**), Pd(P)−$C_6H_4C{\equiv}CPtL_2C{\equiv}CC_6H_4$−Pd(P) (**10**) (Figure SI 6), Pd(P)−$C_6H_4C{\equiv}CPtL_2C{\equiv}CC_6H_4$−Zn(P) (**11**) (Figure SI 7), Zn(P)−$C_6H_4C{\equiv}C$−$PtL_2C{\equiv}CC_6H_4$−Zn(P)−$C_6H_4C{\equiv}CPtL_2C{\equiv}CC_6H_4$−Zn(P) (**12**) and Pd(P)−$C_6H_4C{\equiv}CPtL_2C{\equiv}C$−$C_6H_4$−Zn(P)−$C_6H_4C{\equiv}CPtL_2C{\equiv}CC_6H_4$−Pd(P) (**13**) (Figure SI 8). Typical example of fluorescence decay of compounds **11** and **13** in 2MeTHF at 77 K (red) against the lamp profile (black), typical example of phosphorescence decay of compounds **7** and **8** in 2MeTHF at 77 K (Figure SI 9), and transient absorption spectra in MeTHF at 298 K of Pd(P)−$C_6H_4C{\equiv}CH$ (**3b**), Pd(P)−$C_6H_4C{\equiv}CPtL_2Cl$ (**6**), Pd(P)−$C_6H_4C{\equiv}CPtL_2C{\equiv}CC_6H_6$ (**8**), Pd(P)−$C_6H_4C{\equiv}CPtL_2C{\equiv}CC_6H_4$−Pd(P) (**10**), and Pd(P)−$C_6H_4C{\equiv}CPtL_2C{\equiv}CC_6H_4$−Zn(P)−$C_6H_4C{\equiv}CPtL_2C{\equiv}CC_6H_4$−Pd(P) (**13**) (Figure SI 10). This material is available free of charge via the Internet at http://pubs.acs.org.